UNITED STATES DEPARTMENT OF THE INTERIOR

GEOLOGICAL SURVEY

# MAGNETIC STUDIES OF SELECTED GEOLOGIC AND AEROMAGNETIC FEATURES IN SOUTHWEST SEWARD PENINSULA, WEST-CENTRAL ALASKA

by

John W. Cady and C. L. Hummel

Open-File Report 76-425

1976

This report is preliminary
and has not been edited or
reviewed for conformity with
Geological Survey standards.

CONTENTS

## ILLUSTRATIONS

Figure 7 - Histogram showing measured remanent magnetization and susceptibility. Hatchured areas indicate specimens with the Konigsberger ratio Q (ratio of remanent to induced magnetization) greater than or equal to 1. N is the total number of samples, n the number of samples within the indicated range of susceptibility or remanent magnetization, k the susceptibility, and J the remanent magnetization.

The Appendix contains the profiles aa' through zz" shown in figure 6, as well as profiles (aa') through (jj") from outside the detailed study area. The horizontal scale is approximately 1 inch = 1 mile. The symbol o indicates measured remanent magnetization J; $\Delta$ indicates induced magnetization computed from measured susceptibility and the earth's magnetic field.

# INTRODUCTION

Aeromagnetic anomalies in the western Seward Peninsula show simple patterns of great lateral extent. Our purpose was to identify the sources of the anomalies in the field while detailed geologic mapping was ongoing, so that the aeromagnetic map could be used to extrapolate the geologic mapping into a wider area. Following a brief geological introduction, we focus on the interpretation of aeromagnetic maps in the southwest Seward Peninsula and the presentation of ground magnetometer profiles and magnetic susceptibility and intensity measurements of samples collected along the ground magnetometer profiles.

## Acknowledgments

Fred Walton of the former Marine Geophysics Section of the National Oceanic and Atmospheric Agency made preliminary ground magnetic traverses for these investigations near Nome in 1970. At an early stage of the investigation, Andrew Griscom reviewed the aeromagnetic survey and discussed with Hummel the plan to correlate geologic and aeromagnetic features of the area. W. F. Hanna provided a susceptibility bridge for measuring rock susceptibilities, and took a personal interest in seeing that the measurements were properly made. Personnel of the U.S. Geological Survey rock magnetics laboratory kindly permitted the use of their facilities for sample coring and remanent magnetization measurements.

## GENERAL GEOLOGY

Southwest Seward Peninsula includes elements of nearly all of the major geological features of the Peninsula, and many of these are better represented and exposed there than elsewhere on it. Among these are regionally metamorphosed rocks which make up most of the bedrock, two main groups of structures, two suites of metalliferous lodes associated with them, and widespread surficial deposits and cover. Among the latter are beach, glacial, and alluvial deposits which have yielded placer gold derived from the lodes which has accounted for three-fourths of the mineral production from the entire peninsula.

### Bedrock Geology

The bedrock of the southwest Seward Peninsula can be readily divided into terranes composed mainly of higher and lower grade metamorphic rocks; of these, the former are associated with the youngest structures of the region, whereas the latter contain the only major older structures.

#### Higher grade rocks

Higher, generally amphibolite grade metamorphic rocks, are localized almost entirely in the Kigluaik and Bendeleben Mountain ranges; because the higher grade metamorphites and the igneous rocks in them are best exposed in the Kigluaik Mountains, but are undivided

for the most part, both have been included in the Kigluaik Complex shown on Plate 1.

The Kigluaik Complex consists predominantly of metasediments with subordinate orthogneiss bodies, and includes numerous silicic and mafic dikes and sills. The metasediments comprise gradationally interlayered calc-silicate rocks and marble, quartz and quartz-feldspar biotite schist and quartzite, all more or less graphitic. The contact between the metasedimentary rocks of the higher and lower grade terranes occurs either as a fault or is covered by surficial materials (Plate 1). Despite this, a thick sequence of the lower grade metasediments, which is interpreted to constitute their basal portion, can be correlated with the former on the basis of gross lithology as inferred from mineralogy and physical character. In addition, segments of metasediments occur on both sides of the fault which are similar to the others in bulk composition but are of intermediate metamorphic grade. Together, these indicate that the relationship between the higher grade and basal portion of the lower grade metasediments is a regular, gradational stratigraphic and transitional metamorphic one.

Numerous, generally concordant orthogneiss bodies of all sizes are present throughout the metasediments of the Kigluaik Complex; only the largest of these are shown on Plate 1. Whole rock, Rb/Sr, isotopic ages of 750 m.y. were obtained from two of these bodies near Mt. Osborn (Sainsbury, 1972, p. 2). This indicates that the age of the higher grade metasediments is Precambrian Y and, as such, they are the oldest rocks known on Seward Peninsula.

Lower grade rocks

Nearly all of the bedrock of southwest Seward Peninsula outside the Kigluaik and Bendeleban Mountains is composed of metamorphic rocks of greenschist grade, the only exceptions being sporadic igneous bodies and a few occurrences of still lower grade rocks. The greatest proportion of the lower grade rocks consists of metasedimentary and layered metavolcanogenic rocks of submarine origin. These, in turn, are composed of thick and areally extensive exposures of only a few kinds and suites of rocks; however, the relationships of these rocks are still only imperfectly known. For the purpose of this report, only the fewest of these units needed to delineate the gross character of the bedrock are shown; further, through the selective use of symbols for these units, only those occurrences which have been checked and are in accord with the results of the current field investigations are indicated (Plate 1). The units include the basal graphitic schist and marble unit sequence cited above, the most extensive exposures of two marble units, and two thick sequences of interlayered chloritic schist and marble.

Rocks interpreted to form the basal portion of the lower grade terrane consist of intimately, gradationally interlayered graphitic quartzose, calcareous, and feldspathic chlorite-muscovite schist, quartzite, and marble. As described above, they strongly resemble the high-grade metasediments in gross composition and physical character, and so are inferred to be related to them stratigraphically. The basal graphitic sequence is exposed in four prominent belts; one

extending south from Teller, two north from Nome and Solomon, and a narrower, eastward-trending belt joining the latter south of the Kigluaik Mountains (Plate 1). Along with their presumed higher grade counterparts, rocks belonging to this sequence are thought to be of Precambrian Y age.

Marble of two distinct types--gray and blue-gray, schistose to slabby and massive marble and buff-weathering schistose marble--is ubiquitous throughout all units and all parts of the lower grade terrane. Only the largest exposures of both types are shown on Plate 1. The most extensive exposures of blue-gray marble crop out in a nearly continuous, inverted U-shaped belt between the Snake and Solomon Rivers and south of Salmon Lake (Plate 1). Smaller and more isolated exposures of marble of similar character lie east and west of this belt; for the most part, these exposures are shown as depicted and designated for age by Sainsbury and others (1972, 1972a), especially the largest of these in the western part of the region (Plate 1).

The thickest and most extensive exposure of buff-weathering schistose marble lies in the south-central part of the region. However, a far more widespread exposure of similar marble continues eastward to the Darby Mountains from the small area shown near Council (Miller and others, 1972). Like the contact relations of most of the units in the lower grade terrane, those of the marble have not been determined for certain. Despite this, Sainsbury correlated all of the buff-weathering schistose marble with an argillaceous limestone

which occurs widely throughout northwestern Seward Peninsula (Sainsbury, 1972). The only exposure of this limestone in the area crops out near Teller (Plate 1). Sainsbury assigned a late Precambrian age to this limestone and its metamorphosed equivalents (Sainsbury, 1972, p. 3).

The most widespread and probably the thickest sequences of lower grade metamorphites in southwest Seward Peninsula are composed mainly of feldspathic greenschist and abundant, predominantly gradationally interlayered calcareous and quartzose variants of it; both brown schistose and blue-gray marble, and graphitic quartzite and schist are present throughout the sequences, generally, as sporadic and subordinate beds and members. The most extensive exposure of the greenschist and marble crops out throughout the south-central part of the area. A similar sequence of rocks which occurs in the eastern part of the region was first mapped by Smith in the Solomon area and named the Casadepaga Schist (1910, p. 70); although not so named, the same rocks were extended and further mapped east of this area by Smith and Eakins the following year (1911, p. 40-41). Following Sainsbury, who retained Smith's designation, most of both suites of rocks are thought to be of submarine volcanic and volcanogenic origin and of Precambrian age (Sainsbury, 1972, p. 2).

## Igneous and metaigneous rocks

Igneous and metaigneous rocks occur in both the higher and lower grade terranes of southwest Seward Peninsula. The orthogneiss bodies in the Kigluaik Complex which have yielded wholerock isotopic ages of

750 m.y. are described above. In addition, small to moderate-sized basaltic and granitic dikes and sills are present throughout the Kigluaik Mountains. For the limited purpose of this report, only the single, largest granitic body at the western end of the complex is shown on Plate 1. Sainsbury and others assigned a Cretaceous age to this body (1972, p. 11). The basaltic rocks are most probably of Tertiary age.

In marked contrast with the Kigluaik Complex where examples of neither has been found, gabbroic and metamafic bodies are abundant throughout much of the lower grade terrane. Again, because of the limited purpose of this report, only the gabbro bodies near Teller as shown by Sainsbury (1972), and the largest matamafic body in the central part of the area as mapped by Hummel (1962b) are shown on Plate 1; smaller metamafic bodies, mainly sills, of similar lithologic character, are especially abundant in the greenschist and marble unit. Following Sainsbury and others (1972, p. 10), no age or ages have been assigned to any of the mafic rocks.

Numerous small and a few large metagranitic bodies, nearly all with metatactite zones, occur in a belt between Cape Nome and Salmon Lake (Hummel, 1962a, 1962b); only the body at Cape Nome is shown on Plate 1. The lower grade metagranitic rocks are correlated provisionally with the orthogneiss bodies in the Kigluaik Complex, but no isotopic ages have been obtained from them yet.

Only a very few silicic and basaltic bodies have been found in the lower grade terrane. Like their lithologic equivalents in the

Kigluaik Complex, they are thought to be of Tertiary age, but no direct evidence for this assignment has been determined.

## Structural Geology

Major structures belonging to two systems are represented in southwest Seward Peninsula, and the effects of one of these on the other are such that they can be safely characterized as younger and older. The older structures are also cut by a coordinate set of transcurrent faults and fractures, but the relationship of these to the other younger structures has not been established.

### Older structures

All of the major, older structures which have been identified in southwest Seward Peninsula lie in the lower grade terrane. Although of regional size, they are, in fact, only remnants of once much larger and more extensive structural features which were partially destroyed over the Kigluaik and Bendeleben Mountain ranges and strongly deformed around them (Hummel, 1960, p. B30). The older structures include northward-trending folds, folded thrust faults and sheets, and related petrotectonic features of all sizes produced by concurrent tectonic activity and regional metamorphism. Except where strongly deformed, the older structures are manifested by northward-trending belts of lower grade rocks and gross tectonic and metamorphic features (Plate 1). Correlation of a thick sequence of metasedimentary rocks in the lower grade terrane with others thought to be their higher grade

counterparts in the Kigluaik Mountains was described above. This, in conjunction with structural evidence, provided the basis for regarding these metasediments as the basal portion of the lower grade terrane. Distribution of the basal rocks as mapped throughout the lower grade terrane, has made it possible to delineate four folds which dominate and determine the structural configuration of the lower grade bedrock of southwest Seward Peninsula. Because the contact relationships between the basal and other rock units of lower grade terrane, and among these latter, have not been determined, the resulting folds have been characterized as antiforms and synforms. As manifested mainly by northward-trending belts of basal rocks, the axes of antiforms lie along the Snake and Solomon Rivers, extending respectively north from Nome and Solomon in the central part of the region, and south of Teller in the northwest part (Plate 1). The axis of the synform between the antiforms at Nome and Solomon lies along the Bonanza River. All of these features have been given names to reflect their geographic location, hence the Teller, Snake River, and Solomon River antiforms and the Bonanza River synform.

The only intrinsic evidence bearing on the time of formation of the older structures and related metamorphic features consists of a single isotopic age of ca. 100 m.y. as determined from K/Ar data on biotite (Sainsbury, 1972, p. 7). This coincides with the period of tectonic activity comprising east-west compression and eastward thrusting proposed by Patton and Tailleur (1972), which provides a regional geologic framework that could account for the trend and character of the older structures.

Younger structures

The largest and most obvious younger structure in southwest Seward Peninsula is the Kigluaik Uplift (Hummel, 1960, p. B33) which consists of a horst-like core of higher grade rocks bounded by normal faults (Plate 1); Pleistocene glacial deposits cut by the fault along the north side demonstrate that the uplift is a still active tectonic feature. However, in the context of the region as a whole, the Kigluaik Uplift can be seen to be but one structural element, albeit a major one, on the eastward-trending welt which encompasses both the Kigluaik and Bendeleben Mountain ranges and the bedrock for a considerable distance north of them (Sainsbury, 1972). Within this regional context, other younger structures can also be discerned, as can their effects on the older structures. From this, the Kigluaik Arch can be recognized as a subsidiary structure within the uplift (Plate 1); similarly, the eastward-trending belt of lower grade rocks along the south side of the uplift can be recognized as strongly deformed portions of older, major northward-trending folds. It appears probable from their size that these, in turn, once extended entirely across central Seward Peninsula; if so, only their median portions were uplifted and destroyed over the Kigluaik-Bendeleben welt and deformed remnants of the folds can be expected north of the mountains which correspond to those south of them. As suggested by Grantz (oral commun., 1974), these effects strongly indicate deep-seated, perhaps diapire-driven, tectonic deformation. Such activity may have begun long ago, perhaps as early as late Cretaceous or Tertiary times.

In addition to the Kigluaik Uplift boundary faults, the older structures are also cut and deformed by a series of major, vertical northeast-striking faults and a subordinate but coordinate set of northwest-striking faults and fractures (Plate 1). The largest and most important of these is the Anvil-Hunker fault described earlier by Hummel (1960, p. B35) and the California Creek fault system named here. Provisionally, these faults are thought to be related to Kaltag Fault and so to be of the same age, that is, early to middle Tertiary (Patton and Hoare, 1968, p. D153).

## MAGNETIC STUDIES

### Previous geophysical work

Two aeromagnetic maps cover the land area shown in Figure 1. The northern half was flown with a flight line spacing of 1.2 kilometres and a flight altitude of 300 metres above average terrain (State of Alaska Department of Natural Resources, 1971). The southern half was flown with a flight line spacing of 1.6 kilometres and a flight altitude of 820 metres above sea level, which here gives a terrain clearance of 300 to 600 metres (U. S. Geological Survey, 1969). All flight lines run east-west. In addition, a detailed helicopter magnetic survey with a north-south flight line spacing of 400 metres and an altitude of 60 metres was flown over the beach and adjacent water west of Nome (U. S. Geological Survey, 1969). These aeromagnetic data, for which no interpretations have been published, are presented in detail in Plate 1. A gravity map of the Seward Peninsula by Barnes (1971) was helpful in interpreting the magnetic data.

A ship-borne magnetic survey was made offshore of Nome by the National Oceanographic and Atmospheric Administration, but the data have not been published.

### Geophysical work methods

Aeromagnetic anomalies shown in Figure 1 and Plate 1 were correlated with major geologic features. Ground geophysical studies, conducted primarily within the small rectangular "detailed study area"

outlined in Figure 1 and Plate 1, were used in combination with the aeromagnetic map to construct a map of inferred magnetic-lithologic units (Plate 1) within the area of detailed study. Two-dimensional model studies of major magnetic highs show the inferred subsurface geometry of the top of magnetic rock units (fig. 3, 4, and 5).

Field studies included magnetometer profiling and rock sampling which were intended to accurately locate the boundaries of magnetic rock units, to estimate the relative magnetization of these units, and to determine, if possible, the nature of the magnetic rock and the minerals responsible for its magnetization. Vertical-field magnetometer measurements were made every 20 paces (about 30 metres) along profiles usually alined normal to strike. Instruments used were Jalander and Sharpe fluxgate magnetometers with maximum sensitivities of 10 and 5 gammas, respectively. Breaks between high-amplitude and low-amplitude portions of the ground magnetometer profiles indicate boundaries between strongly and weakly magnetic rock units. Precise location of the boundaries aids in the construction of magnetic models by reducing the number of free variables.

Hand samples of rock were collected for coring and laboratory measurements of susceptibility and remanent magnetization. Samples were collected from most characteristic rock types, but a special attempt was made to sample under local maxima of the ground magnetometer profiles in order to maximize the probability of collecting magnetic samples.

Thin sections have been made from forty of the samples. The location of these samples, all from the detailed study area, are shown by numbered points in Plate 1. The thin sections are retained by C. L. Hummel.

## RESULTS OF AEROMAGNETIC SURVEYS

### Regional description of aeromagnetic data

Computations of depth to magnetic sources indicate that under many of the magnetic highs magnetic rocks must outcrop at the surface. Within the area of Figure 1, magnetic sources can generally be expected to outcrop at the surface, except locally under areas of sedimentary cover.

Four north-south trends of aeromagnetic highs are labeled I in Figure 1 and Plate 1. Part of one of the trends is also labeled A in the detailed study area of Plate 1. These highs generally occur over the graphitic, metasedimentary, lower schist. The highs are flanked by magnetic lows which generally coincide with the marble which overlies the lower schist. Such an alternation of rock types and major magnetic highs and lows reflects the existence of major north-south trending geologic structures south of the Kigluaik Mountains. The irregular character of the magnetic anomalies suggests that the structures are folds rather than rock units with fault boundaries. Mapped Bouguer gravity anomalies (Barnes, 1971) show little correlation with the north-south magnetic anomalies, indicating that the folded rock units lack large density contrasts.

Contrasting with the north-south trending anomalies is an approximately east-west trend of low magnetic relief, labeled J in Figure 1 and Plate 1, which coincides with the Kigluaik and western Bendeleben Mountains. Two belts of subdued highs within this trend,

labeled j, indicate a zone of magnetic rock which, in the Kigluaiks, partly encloses the core of the range. If these highs can be associated with a particular rock type, the wraparound nature of the anomalies may provide a key to understanding structure within the Kigluaiks.

South of the Kigluaiks is a major east-west trending high labeled K. It may continue eastward, greatly subdued to K*. Both the trend of low magnetic relief over the Kigluaiks and the magnetic high (K) south of the Kigluaiks truncate the north-south highs (I). Structures causing the east-west anomalies were probably formed during the uplift of the Kigluaik Mountains. The truncation of the north-south anomalies shows that the north-south structures are older than the Kigluaik uplift.

In Figure 1, dashed lines show lineaments in the aeromagnetic contours which may indicate northwest-southeast and northeast-southwest trending faults. These lines are defined by truncation of or offset of anomalies and occasionally by an alignment of aeromagnetic lows. If these faults exist, they are probably younger than the north-south structures which they cross. Their age, relative to the Kigluaik uplift, cannot be determined because the magnetic discontinuities cannot be traced with any confidence into the areas of low magnetic relief in the Kigluaiks.

Most of the magnetic lows in Figure 1 overlie weakly- to non-magnetic rock. The broadest and deepest of these lows overlie carbonate rock. Other lows occur over schist. Lows labeled N are exceptional, however, in that they are very deep and narrow and do

not occur adjacent to major highs. It is almost certain that these lows are caused by thick bodies of reversely magnetized rock. Other lows which may be caused by reversely magnetized rock are labeled 0.

A broad low labeled M coincides with a 10 mgal gravity low reported by Barnes (1971), and indicates a thick sedimentary section in the Imuruk Basin.

## Magnetic modeling and its interpretation

Two dimensional magnetic models were constructed using the methods of Talwani and Heirtzler (1964) for highs A and B and lows $C_1$, $C_2$, $C_3$, and $C_4$ in Plate 1. High A is one of the north-south highs labeled I in Figure 1, and high B is the east-west high labeled K in Figure 1.

No problems were encountered in removing the regional gradient, which has a minor effect in short profiles. More difficult was the choice of a magnetic datum analogous to the zero-line of the computed magnetic profiles. Datum levels were chosen somewhat arbitrarily to isolate highs from adjoining lows - 515 gammas for high A and the west part of high B, and about 600 gammas (higher due to the regional gradient) around low C. A high datum of 600 gammas was chosen for the east side of high B in order to remove the effects of adjacent, interfering highs. The choice of datum mainly affects estimates of the deep geometry of the causative body. Tests were made with different datum levels to insure that conclusions reached about models do not depend strongly upon choice of datum.

For any given geometry of magnetic source body, a linear least squares solution was used to estimate the magnetization of the body. Assuming uniform magnetization within the body, the anomaly shape usually sufficed to estimate the geometry of the body. Hence, magnetic modeling provided an independent estimate of magnetization which can be compared with estimates derived from rock sampling and ground magnetometer profiles.

## Models for highs A and B

High A (see Figure 3) is caused by a slab-like body of magnetic rock which terminates abruptly in the west under the steep west flank of the high. The slab has a probable thickness of 1 to 3 kilometres. Thicker slabs failed to reproduce the sharp peak at the west side of the high. Deformation of or inhomogeneity within the body of the slab can account for the undulating 10-kilometre-wide east flank of high A. Alternatively, the source could be a thicker body, magnetized non-uniformly, having a highly magnetic zone under the west peak and a broad, less-magnetic zone about 10 kilometres wide under the undulating east flank of the high.

Modeling of the aeromagnetic data and the ground magnetometer profiles jj' and jj'' both show that the slab emerges at the surface along its west boundary. The boundary occurs on low tundra-covered slopes east of the Penney River as far north as latitude $64^{o}40'$. At this point, the boundary crosses the river and runs to the north towards hill 1961, passing just east of hill 2000+. Because high A

and the inferred magnetic boundary are continuous across the Penney River, no major fault can lie along the headwaters of the Penney River. More likely the west boundary of the slab is a major fault which crosses the Penney River. Magnetic schist east of the fault is juxtaposed against carbonate rocks and less magnetic schist west of the fault.

North of hill 1961, high A is offset about 4 kilometres to the east, possibly by a northwest-southeast striking fault.

High B (see sections $B_1B_2$ and $B_3B_4$ in Figure 4) is caused by a body of magnetic rock which widens with depth and extends to a depth of 5 to 9 kilometres or more. Its base is therefore much deeper than the source for high A.

Profile $B_1B_2$, made across the narrowest part of high B, indicates a highly magnetic source body, about 1 kilometre wide, which must outcrop at the surface. Interference from other nearby highs makes any determination of subsurface geometry uncertain, but there is some indication that the body dips steeply to the north. The top of the body determined from aeromagnetic modeling lies nearly one kilometre south of the top of the body determined from the ground magnetometer profile.

Profile $B_3B_4$, made across the widest part of high B, shows that here the body is up to 3 kilometres wide near its top. The body widens with depth to the north and south.

The proximity of highs A and B, their roughly similar amplitudes, and the fact that they both occur over the lower, graphitic schist,

suggests that they are caused by related sources. The body causing high B, however, has a much greater depth extent than the body causing high A. A possible explanation is that a slab of magnetic schist, 1 to 3 kilometres thick, is present at a depth of 5 to 10 kilometres over much of the area with high magnetic relief shown in Figure 1 and Plate 1. Under the highs labeled I, the magnetic schist approaches the surface in gentle anticlines. Under high A an anticline is faulted along its west flank, causing an uplifted but essentially horizontal slab of magnetic schist east of the fault to be juxtaposed against carbonate rocks and weakly magnetic schists west of the fault.

In contrast, under high B the magnetic schist does not occur as an upward faulted sub-horizontal slab. Instead, it has been abruptly tilted upward by the uplift of the Kigluaiks. It retains its deep roots, thus causing a broader and higher amplitude magnetic high. Tectonic thickening, or possibly metamorphic changes, may also account for the greater volume of magnetic schist adjacent to the Kigluaiks. The high labeled L may be a similar upturned slab of schist north of the Kigluaiks.

### Models for lows labeled C

Aeromagnetic lows C1, C2, and the eastern part of C3 coincide with carbonate rocks, primarily marble. Schist crops out beneath the center of low C3, but the low suggests that the marble dips to the west beneath this schist. Low C4 occurs in the same trend as lows C1 and C2, suggesting that marble is present beneath the alluvium at C4.

Interference from adjoining highs makes it difficult to interpret the lows quantitatively. Comparison of anomaly shapes with those published by Andreasen and Zietz (1969, plates 119C, 161C, and 203C) suggest that the marble bodies under lows C1, C2, and C4 extend to a depth of roughly 1 kilometre below sea level. The inferred carbonate body beneath low C3 may have a bottom as deep as 3 kilometres or more.

The presence of lows over carbonate bodies contrasts sharply with the situation at X near the east side of Figure 1 and Plate 1 where a large mapped area of limestone coincides with a weak magnetic high. From geologic mapping (Sainsbury, Hudson, Ewing, and Marsh, 1972), it is inferred that the limestone at X occurs in a thrust sheet too thin to cause an aeromagnetic low.

One elongate aeromagnetic low occurring over marble was modeled along $C_1C_2$ to provide an independent check on the depth extent of marble bodies. The model, shown in Figure 5, has bodies of weakly magnetic schist extending to infinity on either side, and a body of non-magnetic marble under the low. Least-squares solutions yield magnetizations in the schist of $42 \times 10^{-5}$ gauss for body 1 and $63 \times 10^{-5}$ gauss for alternate body 2.

In the simplified model, narrow flanking highs to either side of the low imply that the marble body is a wedge-like body one kilometre or less thick, like body 1 in Figure 5. The aeromagnetic map shows, however, that these flanking highs are due in part to zones of high magnetization in the schist. Hence, it is possible for the marble body to be a prism-shaped body with a depth extent of several kilometres.

Study of aeromagnetic lows has not led to firm conclusions about the thickness of carbonate bodies. The best guess is that carbonate bodies, when they are accompanied by 40 to 70 gamma aeromagnetic lows, are at least one, and possibly more than three, kilometres thick. Carbonate bodies not accompanied by aeromagnetic lows are thinner and may be subhorizontal thrust sheets.

## RESULTS OF GROUND MAGNETIC STUDIES

Locations of ground magnetometer traverses are shown by lines aa' through zz" and (aa') through (jj") in Plate 1. Dots along these lines are sample sites. All of the ground magnetometer profiles, at an approximate scale of 1 inch = 1 mile, are presented in the appendix along with graphs showing the susceptibility and remanent magnetization of samples collected along the profiles. In addition, ground magnetometer profiles from the detailed study area are presented all together at reduced scale in Figure 6.

### Magnetic properties of rocks

Laboratory measurements of susceptibility and remanent magnetization were made on cores taken from about 300 hand specimens. In addition, susceptibility was measured in 12 soil samples taken beneath some of the major aeromagnetic highs. The results of these measurements are plotted as histograms in Figure 7. Two-thirds of the samples are from the detailed study area shown in Plate 1; the rest are from neighboring areas. An attempt was made to sample all representative rock types. Sampling was most intense, however, in the schistose metasedimentary rocks which underlie the major aeromagnetic highs.

Susceptibility of cores was measured in an external magnetic field of 1,000 Hz and a peak amplitude of 0.5 oersted (Hanna, W. F., written commun., 1973). Most of the cores were drilled perpendicular to cleavage, and susceptibility was measured only along this direction. Susceptibility measured parallel to cleavage in some of the cores with

higher susceptibilities was found to be up to 30 percent greater. Hence, the average susceptibility of the samples may be 10 to 20 percent greater than that indicated in Figure 7. Susceptibility of soil samples was measured in a commercial susceptibility bridge using an external magnetic field of 1,000 Hz and a peak amplitude of 1.0 oersted. Remanent magnetization of the samples was measured in a spinner magnetometer described by Doell and Cox (1965).

Magnetic modeling results show that a magnetization of $140 \times 10^{-5}$ gauss is needed to explain aeromagnetic high A, which has a typical amplitude of 400 gammas. High B, with an amplitude of 500 to 700 gammas, requires a body with magnetization ranging from 120 to $430 \times 10^{-5}$ gauss. Local peaks in the ground magnetic profiles shown in Figures 3, 4, and 6 have amplitudes of 500 to 2,000 gammas. These peaks are caused both by inhomogeneities in magnetic properties of the underlying rocks and by local topographic effects. Whatever their sources, these local anomalies require magnetizations of 100 to $1,000 \times 10^{-5}$ gauss.

Figure 7 shows that most of the rock samples are far too weakly magnetic to cause the observed aeromagnetic or ground magnetic highs. The greatest susceptibility measured is only $87 \times 10^{-5}$ gauss/oersted. This susceptibility yields an induced magnetization of $45 \times 10^{-5}$ gauss in an ambient field of 0.55 oersted. Only 11 samples have remanent magnetizations greater than $100 \times 10^{-5}$ gauss. Only one of these samples (from station 60 in line $A_1A_2$) underlies either high A or high B in Plate 1. Eight of these eleven magnetic samples occur under minor aeromagnetic highs near Basin Creek and King Mountain (ground profiles uu' and yy' in Plate 1 and Figure 6.

One reason why highly magnetic rocks were not found is that high A, and to a lesser extent high B, occur over soil-covered slopes which have very few outcrops compared to adjacent ridges. In detail, many of the ground magnetic highs occur over grassy swales, while lows occur over adjacent outcrops. These observations suggest that the rocks which are magnetic are also particularly vulnerable to erosion. Another factor is suggested by the very noisy character of many ground magnetometer profiles. Magnetic material, instead of being uniformly distributed throughout a massive body, may be concentrated in narrow zones which are hard to locate in areas of poor exposures.

Even though highly magnetic rock was not found under highs A and B, it is clear that the gross rock unit or units responsible for the highs are represented by some of the samples. Samples were taken in places where steep magnetic gradients show that magnetic rocks must come to within 10 to 30 metres of the surface. Many of the samples contained abundant hematite. Preliminary petrographic examination of 25 thin sections by Travis Hudson (written commun., 1972) showed that 10 to 80 percent of the opaque minerals in half of the samples are secondary and post-metamorphic. It is tempting to speculate, pending a more thorough petrographic study, that weathering has oxidized magnetite to hematite near the surface, and at a depth of 20 to 30 metres, fresh magnetite is present to cause the magnetic anomalies.

### Map of inferred magnetic lithologies

Three kinds of map patterns in the detailed study area of Plate 1 show the inferred extent of outcropping bodies of highly and moderately

magnetized rock. Wherever possible, ground magnetometer profiles were used to locate the boundaries of these rock bodies. The boundaries were interpolated and extrapolated using the aeromagnetic map.

Major exposures of magnetic rock underlie highs A and B. In each case the map pattern shows only the exposed tip of a much larger body. Lesser highs, possibly covered by the same rocks that produce magnetic high A, are labeled D in Plate 1. Other lesser anomalies are labeled E, F, G, H, I, and J. In the following discussion, closed highs and lows are identified by the gamma-value printed at the closure. A north-south trending group of highs labeled D occurs over schist west of high A. Ground magnetometer profiles bb' and cc' over high D-685 are very noisy, similar in character to profiles over highs A and B. Hence, the inferred magnetic rock unit under high D is shown with the same map pattern as that used under highs A and B. High D could be caused by a vertical prism of schist, inhomogeneous and highly magnetic in zones, similar to that which causes high A. The amplitude of high D is lower because the causative body is only about one kilometre wide. Highs labeled E, also over schist, are much weaker than highs A or D and probably indicate a different rock unit. Ground magnetometer profile ff' shows that here the rocks are an order of magnitude less magnetic than those under high D-685. East of high A occurs another group of highs, also over schist, labeled F, nearly as high as the noise levels measured over high A, suggesting that high F could be caused by small bodies of the same rock type which causes high A. The inferred source rocks of highs E and F are shown by identical map patterns, but the rock types under them probably are not identical.

Interspersed with the local highs labeled F, and also over schist, occur local lows labeled G. The east end of ground magnetometer profile ww' passes onto the south end of low G-469. An abrupt transition between high and low noise levels on the profile indicates a boundary between magnetic and non-magnetic schist. The alternating pattern of highs labeled F and lows labeled G probably delineates bodies of two different kinds of schist.

Highs labeled H correlate quite closely with the upper chloritic schist labeled pGg on Plate 1. All mapped occurrences of pGg do not produce aeromagnetic highs, however, so there must be more than one variety of pGg. The largest occurrence of pGg with no associated aeromagnetic high is at Newton Peak, 10 kilometres northeast of Nome. Eight of the eleven samples in which we found remanent magnetization to be greater than $100 \times 10^{-5}$ gauss came from the metagabbro unit along ground magnetometer profiles uu' and yy'. Rocks with measured remanent magnetizations of 100 to $200 \times 10^{-5}$ gauss can easily produce the ground magnetometer noise levels of 200 to 800 gammas observed along these profiles. Hand specimens of this highly magnetic unit appear to be felsic metavolcanic rock. The patchiness of the magnetic highs suggests that magnetic rock occurs as isolated pods in the pGg unit.

A low labeled B' north of high B is the complimentary low to high B. It does not indicate reversely magnetized rock.

Ground magnetometer profiles xx' and yy' were made across a known southwest- to northeast-trending Anvil-Hunker fault. This fault

coincides with a lineation on the aeromagnetic map. The fault occupies zones of low noise in both ground profiles, but there is nothing in the profiles which can be identified as a magnetic "signature" of the fault.

A fault containing sulfide-bearing schist was located by a very narrow, 2,000 gamma spike at sample site 92 on ground magnetometer profile cc'. The spike is so narrow that it would barely be detectable in an aeromagnetic survey.

## SUMMARY AND CONCLUSIONS

The western Seward Peninsula is crossed by major north-south structures, probably folds, which locally bring magnetic schist (the graphitic lower schist) close to the ground surface, causing north-south trending aeromagnetic highs. These structures, and the magnetic anomalies they cause, are truncated by the east-west trending Kigulaik Mountains. Just south of the Kigluaiks, magnetic schist was upturned and brought to the surface during the uplift of the mountains. This schist now gives rise to a major east-west aeromagnetic high. The inferred extent of outcrop of these magnetic bodies is shown by a horizontally lined map pattern in Plate 1.

Magnetic modeling shows that one of the north-south highs (A in Plate 1) is caused by the western edge of a thin, subhorizontal slab-like body, while the east-west high south of the Kigluaiks (B in Plate 1) is caused by a body with deep roots. Both may contain the same rock type, but they have undergone different kinds of deformation.

Aeromagnetic lows occur over carbonate rocks. The calculated thickness of carbonate bodies causing lows is roughly one kilometre. Thinner carbonate bodies, possibly thrust sheets, do not produce aeromagnetic lows.

None of more than 300 rock samples collected had susceptibilities high enough to cause the observed magnetic highs and less than 10 percent of the samples showed remanent magnetizations high enough to cause the observed anomalies. Most of the strongly magnetic samples were found

distant from the major aeromagnetic highs. Ground magnetometer profiles showed, however, that highly magnetic rock lies within 10 to 30 metres of the surface beneath aeromagnetic highs. Possibly weathering has oxidized magnetite to hematite in the top 10 to 30 metres.

## REFERENCES


Andreasen, G. E., and Zietz, Isadore, 1969, Magnetic fields for a 4 x 6 prismatic model: U.S. Geol. Survey Prof. Paper 666, 9 p., 210 pl.

Barnes, D. F., 1971, Preliminary Bouguer anomaly and specific gravity maps of Seward Peninsula and Yukon Flats, Alaska: U.S. Geol. Survey open-file report.

Doell, R. R., and Cox, A., 1965, Measurement of the remanent magnetization of igneous rocks: U.S. Geol. Survey Bull. 203-A, p. 1-32.

Hummel, C. L., 1960, Structural geology and structural control of mineral deposits near Nome, Alaska, in Short papers in the geological sciences: U.S. Geol. Survey Prof. Paper 400-B, p. B30-B33.

_____, 1962a, Preliminary map of the Noma C-1 quadrangle, Seward Peninsula, Alaska: U.S. Geol. Survey Mineral Inv. Field Studies Map, MF-247.

_____, 1962 b, Preliminary geologic map of the Nome D-1 quadrangle, Seward Peninsula, Alaska: U.S. Geol. Survey Mineral Inv. Field Studies Map, MF-248.

Johnson, G. R., and Sainsbury, C. L., 1974, Aeromagnetic and generalized geologic map of the west-central part of the Seward Peninsula, Alaska: U.S. Geol. Survey Map GP-881.

Miller, T. P., Grybeck, D. G., Elliott, R. L. and Hudson, Travis, 1972, Preliminary geologic map of the eastern Solomon and southeastern Bendelen quadrangles, eastern Seward Peninsula, Alaska: U.S. Geol. Survey open-file report, scale 1:250,000.

Moffit, F. H., 1913, Geology of the Nome and Grand Central quadrangles, Alaska: U.S. Geol. Survey Bull. 533, 140 p.

Patton, W. W., Jr., and Tailleur, I. L., 1972, Evidence in the Bering Strait region for differential movement between North America and Eurasia: Abs. Geol. Soc. of Amer. 1972 Ann. Mtg., Nov., 1972.

Sainsbury, C. L., 1972, Geologic map of the Teller quadrangle, western Seward Peninsula, Alaska: U.S. Geol. Survey Misc. Geol. Inv. Map, I-685.

_____, 1974, Geologic map of the Bendeleben quadrangle, Seward Peninsula, Alaska: Anchorage, AK, The Mapmakers, 31 p., 1:250,000 scale map.

Sainsbury, C. L., Hummel, C. L., and Hudson, Travis, 1972, Reconnaissance geologic map of the Nome quadrangle, Seward Peninsula, Alaska: U.S. Geol. Survey open-file report, 28 p.

Sainsbury, C. L., Hudson, Travis, Ewing, R., and Marsh, W. R., 1972a, Reconnaissance geologic map of the west half of the Solomon quadrangle, Alaska: U.S. Geol. Survey open-file report, 10 p.

_____, 1972b, Reconnaissance geologic maps of the Solomon D-5 and C-5 quadrangles, Seward Peninsula, Alaska: U.S. Geol. Survey open-file report, 12 p.

Sainsbury, C. L., Hudson, Travis, Ewing, R., and Richards, Thomas, 1972c, Reconnaissance geologic map of the Solomon D-6 quadrangle, Seward Peninsula, Alaska: U.S. Geol. Survey open-file report, 17 p.

Smith, P. S., 1910, Geology and mineral resources of the Solomon and Casa de paga quadrangles, Seward Peninsula, Alaska: U.S. Geol. Survey Bull. 433, 234 p.

Smith, P. S., and Eakin, H. M., 1911, A geologic reconnaissance in southeastern Seward Peninsula and the Norton Bay-Nulato region, Alaska: U.S. Geol. Survey Bull. 449, 146 p.

Talwani, M., and Heirtzler, J. R., 1964, Computation of magnetic anomalies caused by two dimensional structures of arbitrary shape, in Parks, G., ed., Computers in the mineral industries: Stanford, Calif., Stanford Univ., p. 464-480.

U.S. Geological Survey, 1969, Airborne geophysical surveys in Seward Peninsula area, Alaska: U.S. Geol. Survey open-file report.

West, W. S., and Matzko, J. J., 1953, Reconnaissance for radioactive deposits in the vicinity of Cape Nome, 1947, in Reconnaissance for radioactive deposits in the vicinity of Teller and Cape Nome, Seward Peninsula, Alaska, 1946-47: U.S. Geol. Survey Circ. 244, p. 5-8.

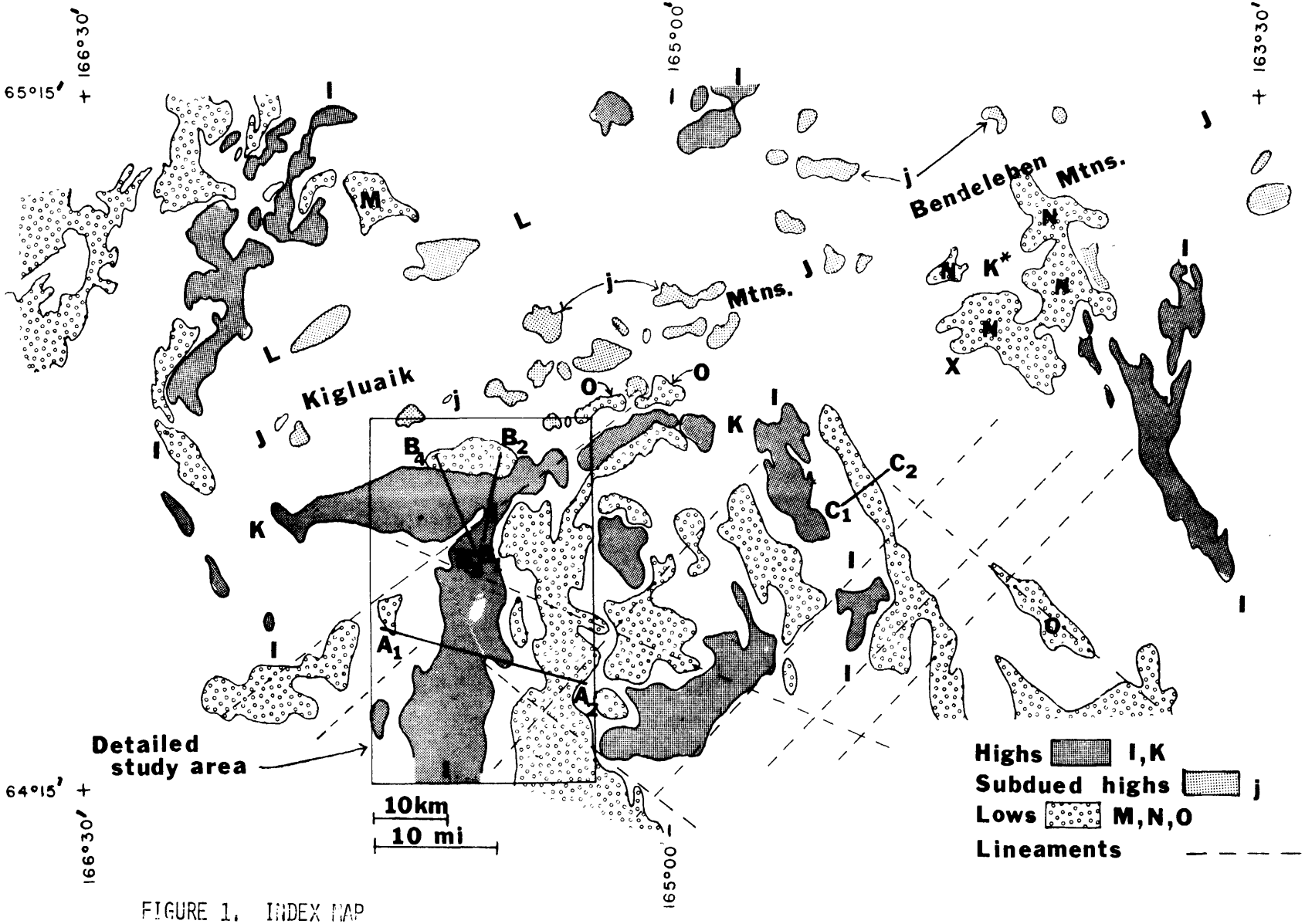


FIGURE 1. INDEX MAP

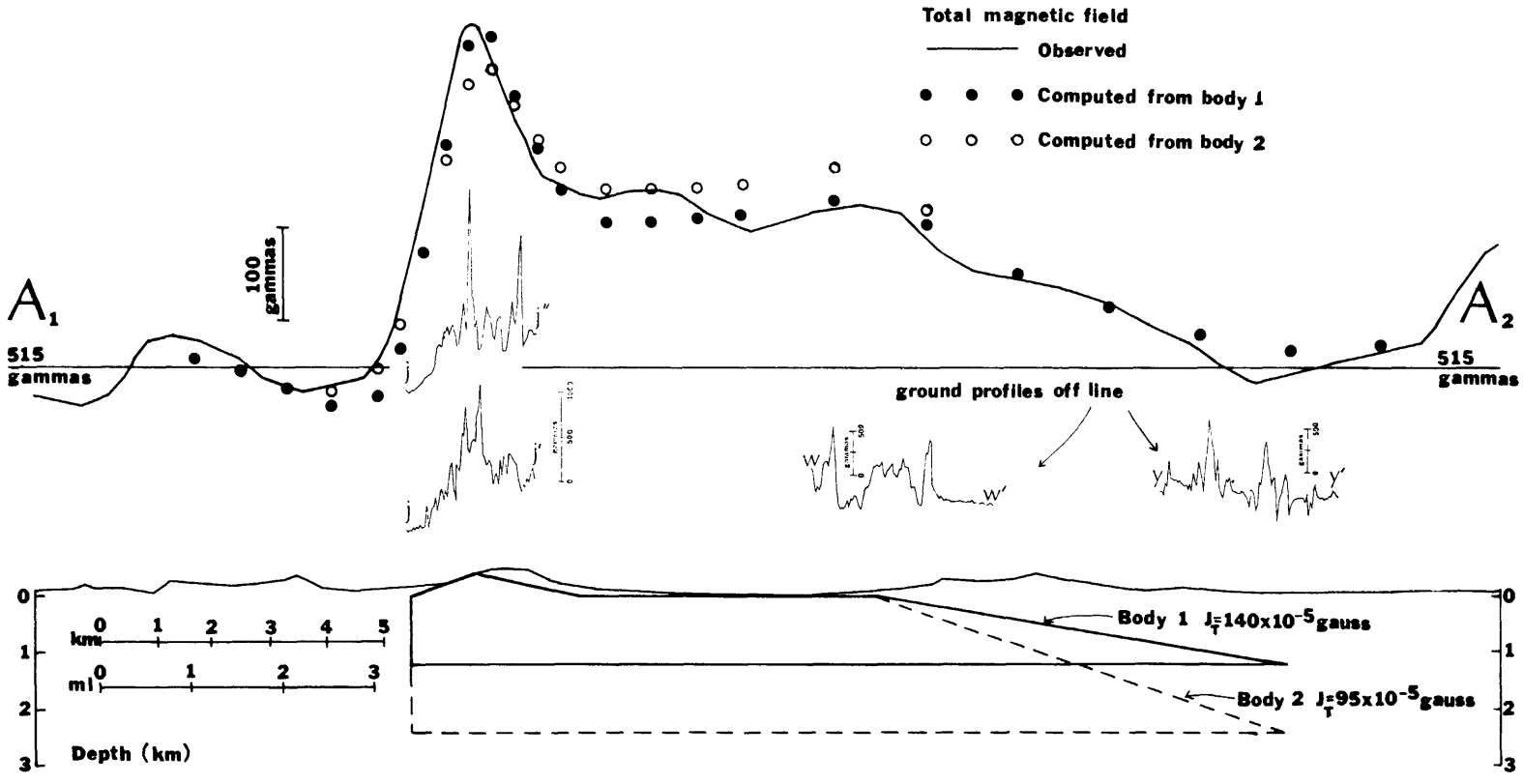


FIGURE 3. TWO-DIMENSIONAL MAGNETIC MODEL FOR THE PENNY RIVER HIGH (HIGH A). $J_T$ IN THIS AND FIGURES 4 AND 5 IS THE INFERRED TOTAL MAGNETIZATION (REMANENT PLUS INDUCED) ASSUMED PARALLEL TO THE EARTH'S MAGNETIC FIELD.

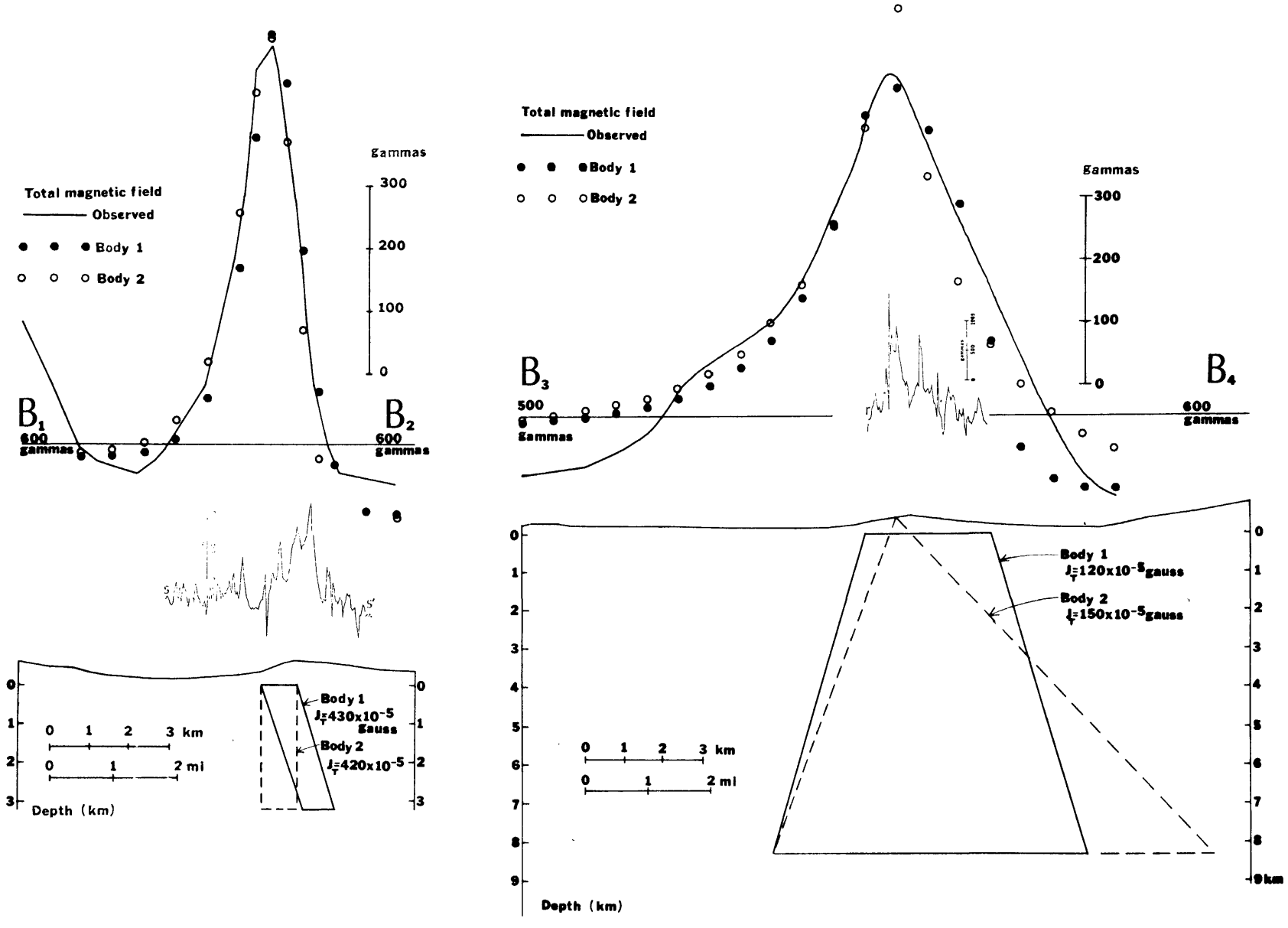


FIGURE 4. TWO-DIMENSIONAL MAGNETIC MODELS FOR THE HIGH SOUTH OF THE KIGLUAIK MOUNTAINS (HIGH ), $J_T$ IS INFERRED TOTAL MAGNETIZATION.

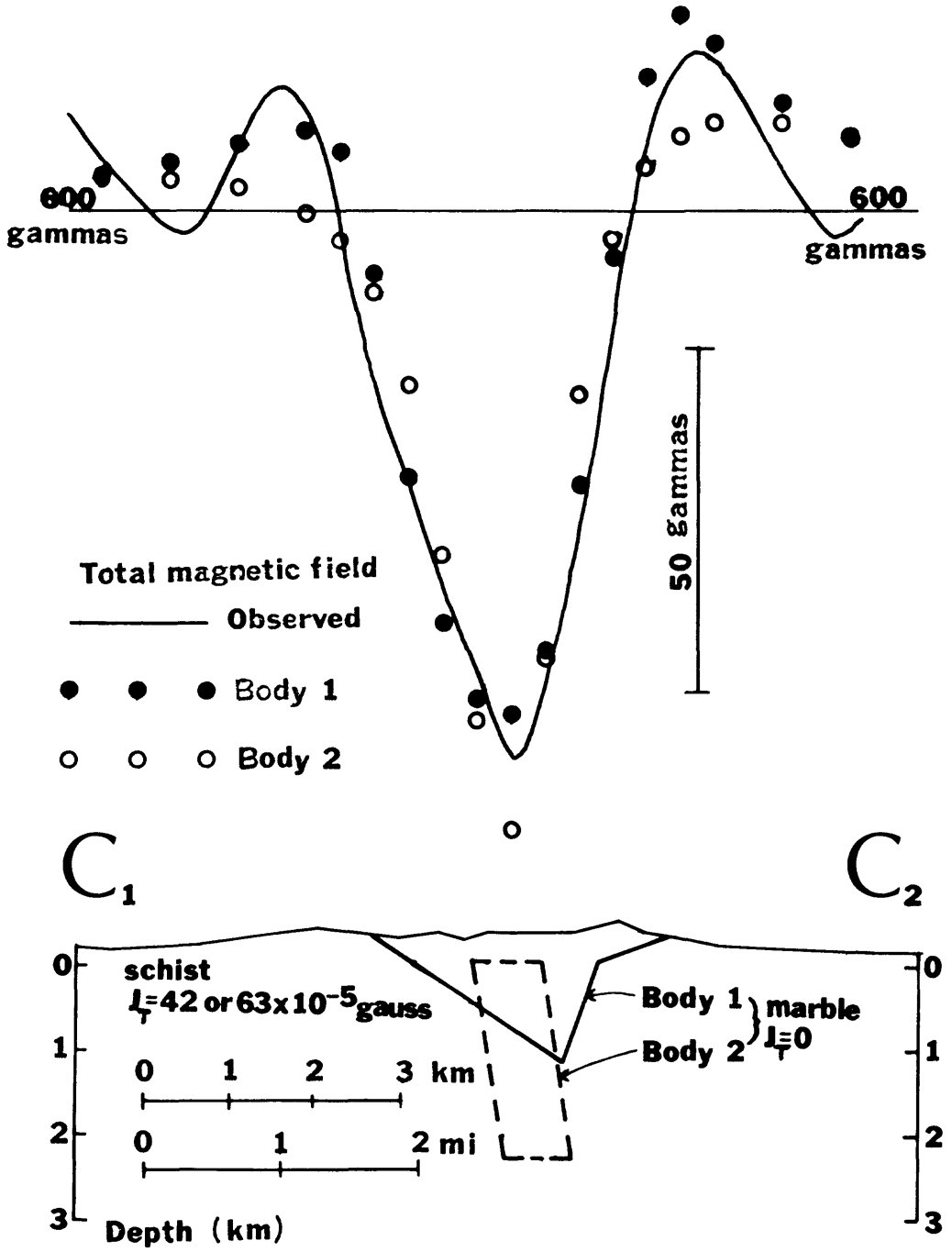


FIGURE 5. TWO-DIMENSIONAL MAGNETIC MODEL ALONG PROFILE $C_1C_2$ FOR THE LOW OVER A CARBONATE BODY. MAGNETIZATION OF COUNTRY ROCK (SCHIST) IS $42 \times 10^{-5}$ GAUSS AROUND BODY 1 AND $63 \times 10^{-5}$ GAUSS AROUND BODY 2. $J_T$ IS INFERRED TOTAL MAGNETIZATION.

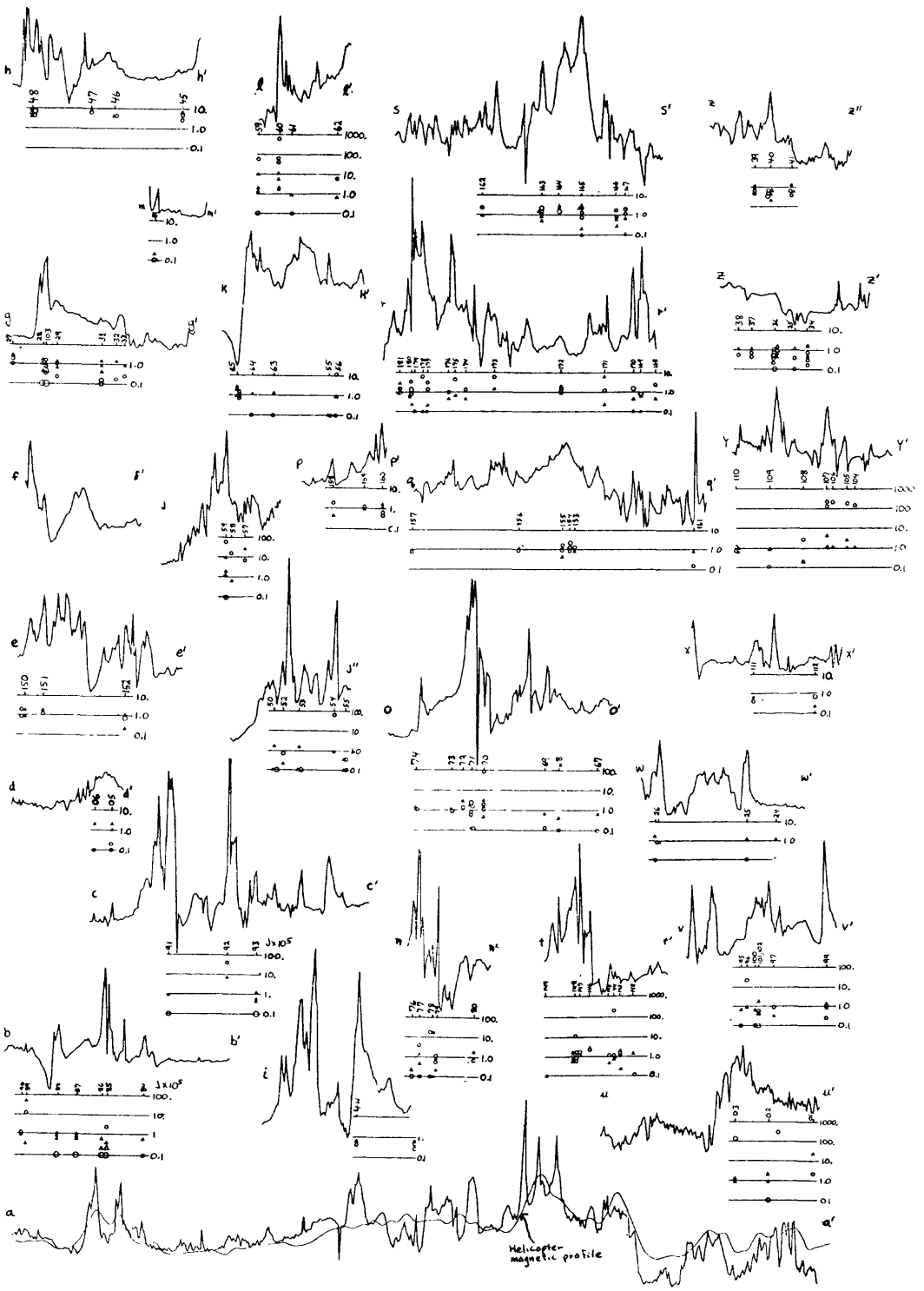


FIGURE 6. GROUND MAGNETOMETER PROFILES ALONG TRAVERSE LINES SHOWN IN DETAILED STUDY AREA OF FIGURE 2. BENEATH PROFILES ARE GRAPHS SHOWING NUMBERED SAMPLE LOCATIONS, MEASURED REMANENT MAGNETIZATION (CIRCLES), AND INDUCED MAGNETIZATION COMPUTED FROM MEASURED SUSCEPTIBILITY (TRIANGLES). SEE APPENDIX FOR EXPANDED VIEWS OF PROFILES.

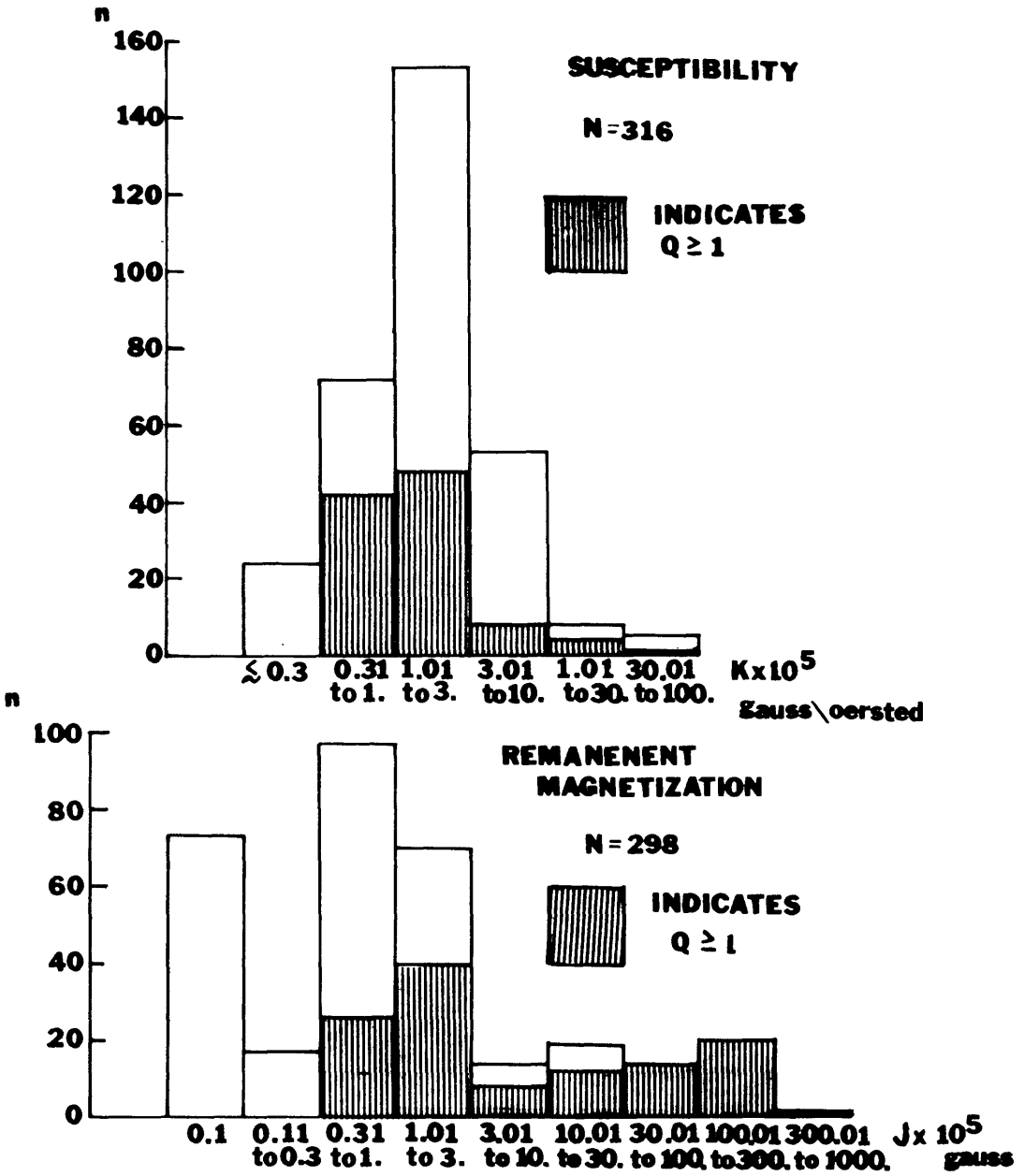


FIGURE 7. HISTOGRAM SHOWING MEASURED REMANENT MAGNETIZATION AND SUSCEPTIBILITY. HACHURED AREAS INDICATE SPECIMENS WITH THE KONIGSBERGER RATIO Q (RATIO OF REMANENT TO INDUCED MAGNETIZATION) GREATER THAN OR EQUAL TO 1. N IS THE TOTAL NUMBER OF SAMPLES, n IS THE NUMBER OF SAMPLES WITHIN THE INDICATED RANGE OF SUSCEPTIBILITY OR REMANENT MAGNETIZATION, κ IS THE SUSCEPTIBILITY, AND J THE REMANENT MAGNETIZATION.

THE APPENDIX CONTAINS THE PROFILES AA' THROUGH ZZ" SHOWN IN FIGURE 6, AS WELL AS PROFILES (AA') THROUGH (JJ") FROM OUTSIDE THE DETAILED STUDY AREA. THE HORIZONTAL SCALE IS APPROXIMATELY 1 INCH = 1 MILE. THE SYMBOL o INDICATES MEASURED REMANENT MAGNETIZATION J; ▲ INDICATES INDUCED MAGNETIZATION COMPUTED FROM MEASURED SUSCEPTIBILITY AND THE EARTH'S MAGNETIC FIELD.

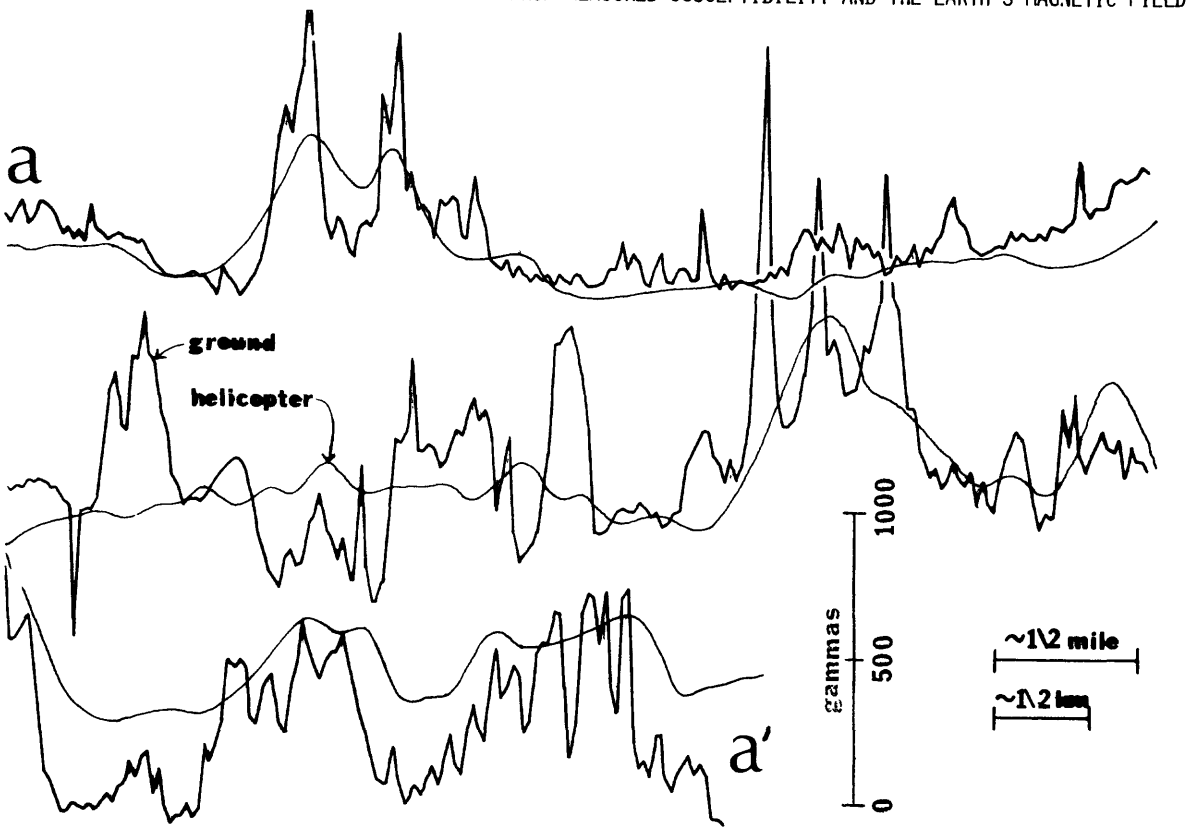


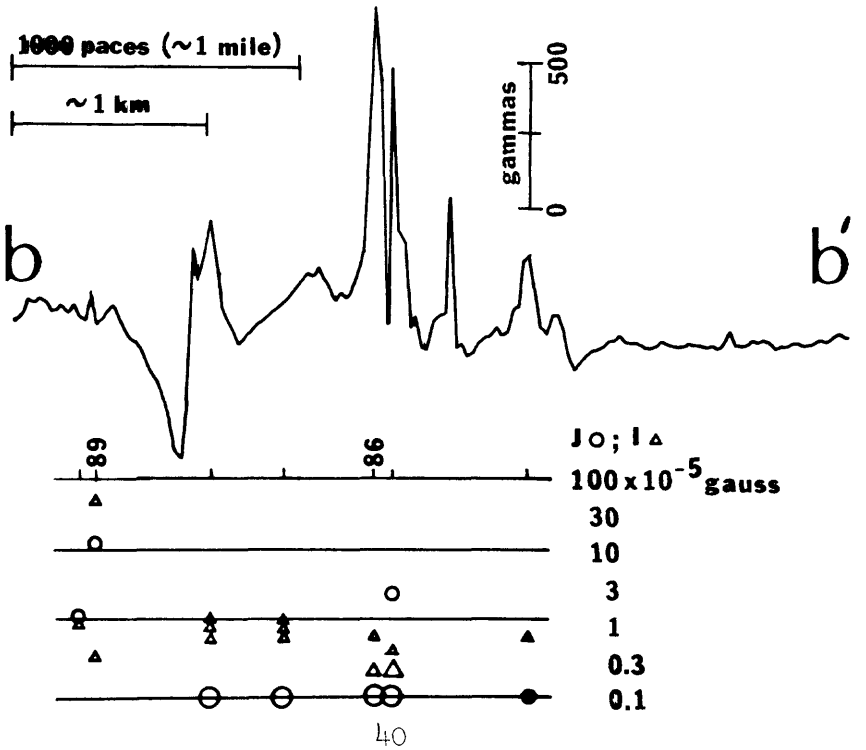

gammas
0
500
1000
1000 paces (~1 mile)
~1 km
C
C'
92
Jo; I△
100 x 10^-5 gauss
30
10
3
1
0.3
0.1
d
d'
e
e'
500
0
gammas
1000 paces (~1 mile)
~1 km
Jo; I△
10 x 10^-5 gauss
3
1
0.3
0.1

h'
h
i'
i
gammas
0
500
1000
10 x 10-5
3 gauss
1
0.3
0.1
48
44
~½ mile
~½ km
f'
f
g'
g
1000 paces (~1 mile)
~ 1 km
3 x 10-5 gauss
103

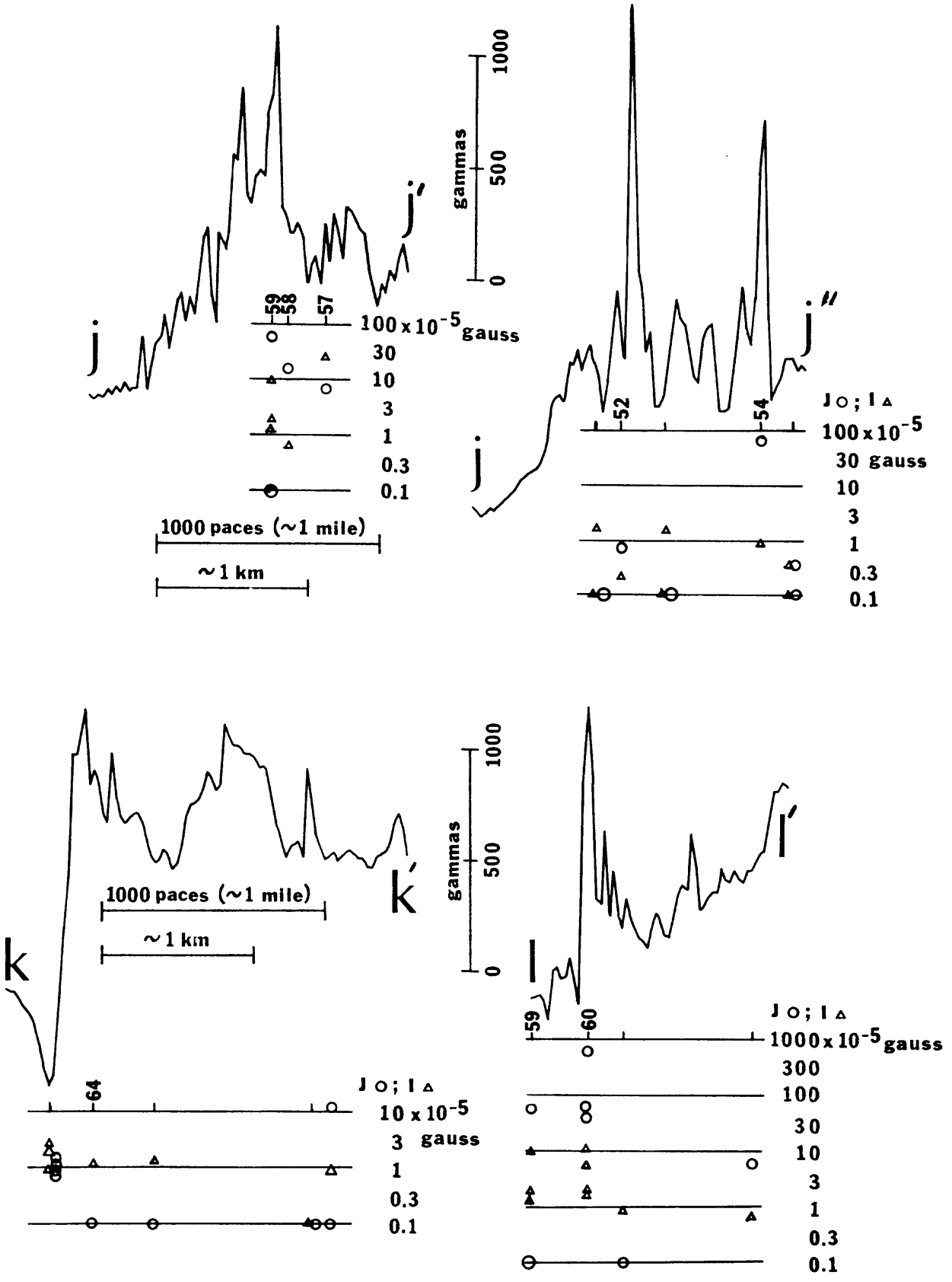
j
j'
gammas
1000
500
0
59
58
57
100 x 10-5 gauss
30
10
3
1
0.3
0.1
1000 paces (~1 mile)
~1 km
j''
52
54
J ○; I △
100 x 10-5
30 gauss
10
3
1
0.3
0.1
k
k'
1000 paces (~1 mile)
~1 km
64
J ○; I △
10 x 10-5
3 gauss
1
0.3
0.1
l
l'
59
60
J ○; I △
1000 x 10-5 gauss
300
100
30
10
3
1
0.3
0.1

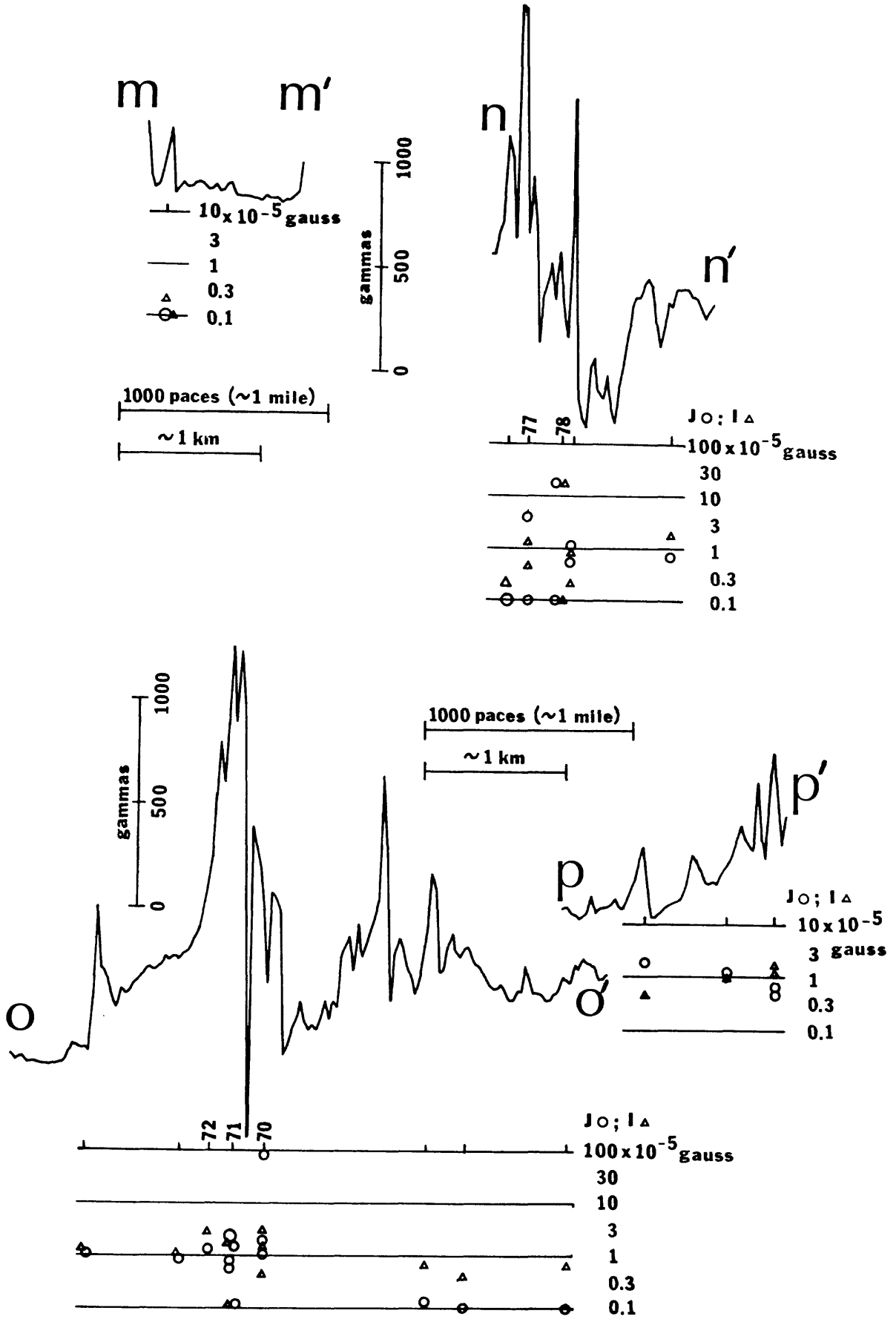
m
m′
10x 10-5gauss
3
1
0.3
0.1
gammas
1000
500
0
1000 paces (~1 mile)
~1 km
n
n′
77
78
J○; I△
100x10-5gauss
30
10
3
1
0.3
0.1
o
o′
72
71
70
p
p′
10x10-5
3 gauss
1
0.3
0.1

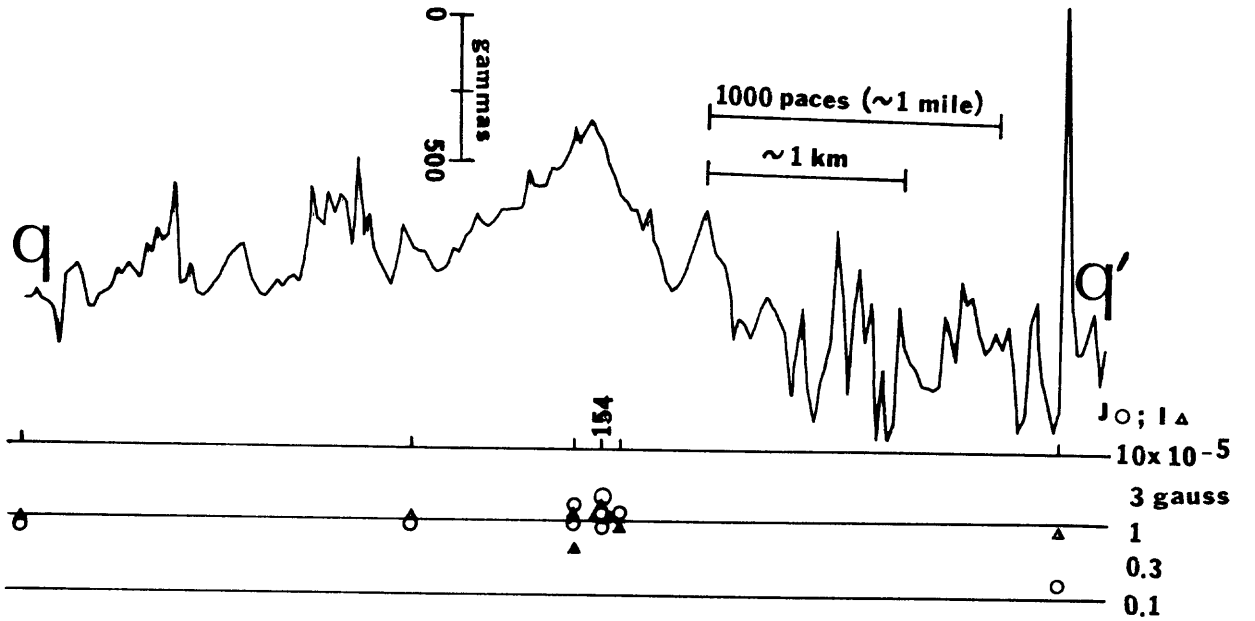
0
500
gammas
1000 paces (~1 mile)
~1 km
q
q′
154
J ○; I △
10x 10⁻⁵
3 gauss
1
0.3
0.1

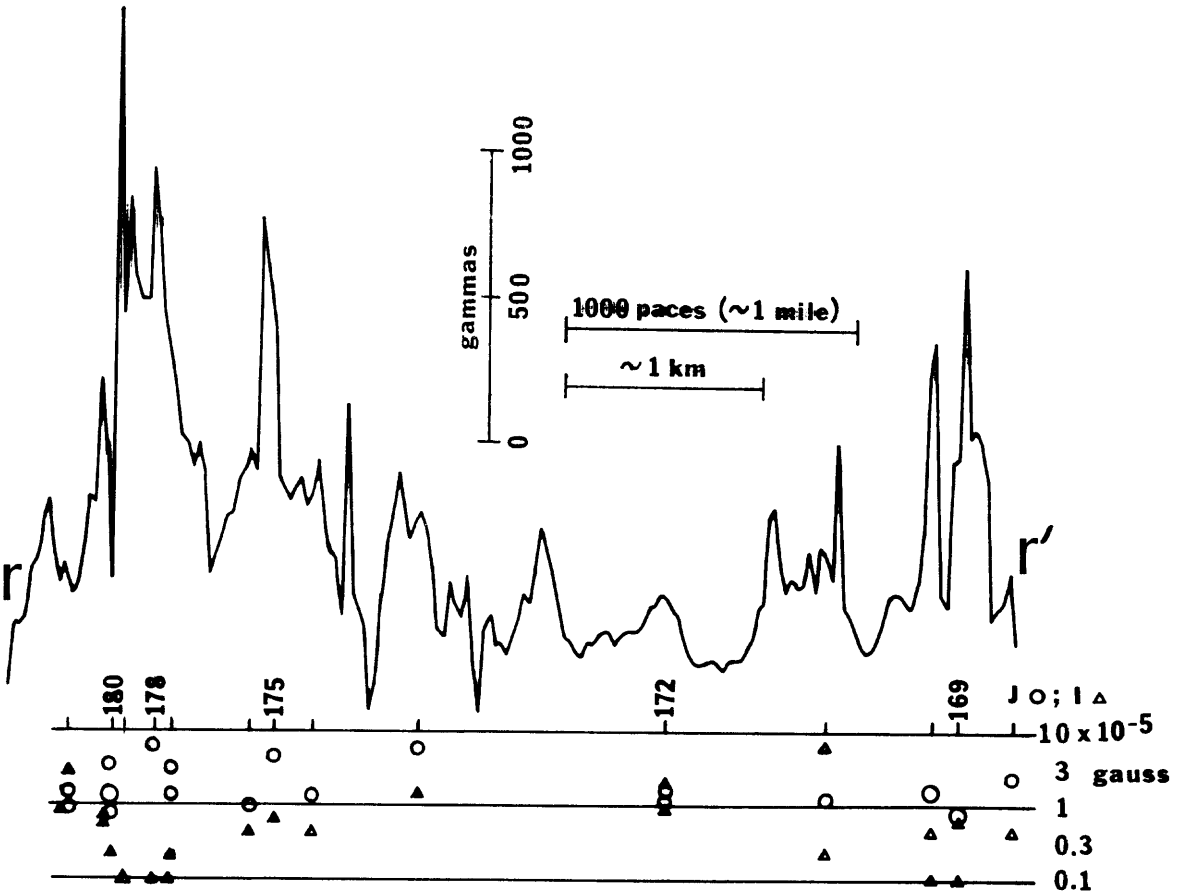
1000
500
0
gammas
1000 paces (~1 mile)
~1 km
r
r′
180
178
175
172
169
J ○; I △
10 x 10⁻⁵
3 gauss
1
0.3
0.1

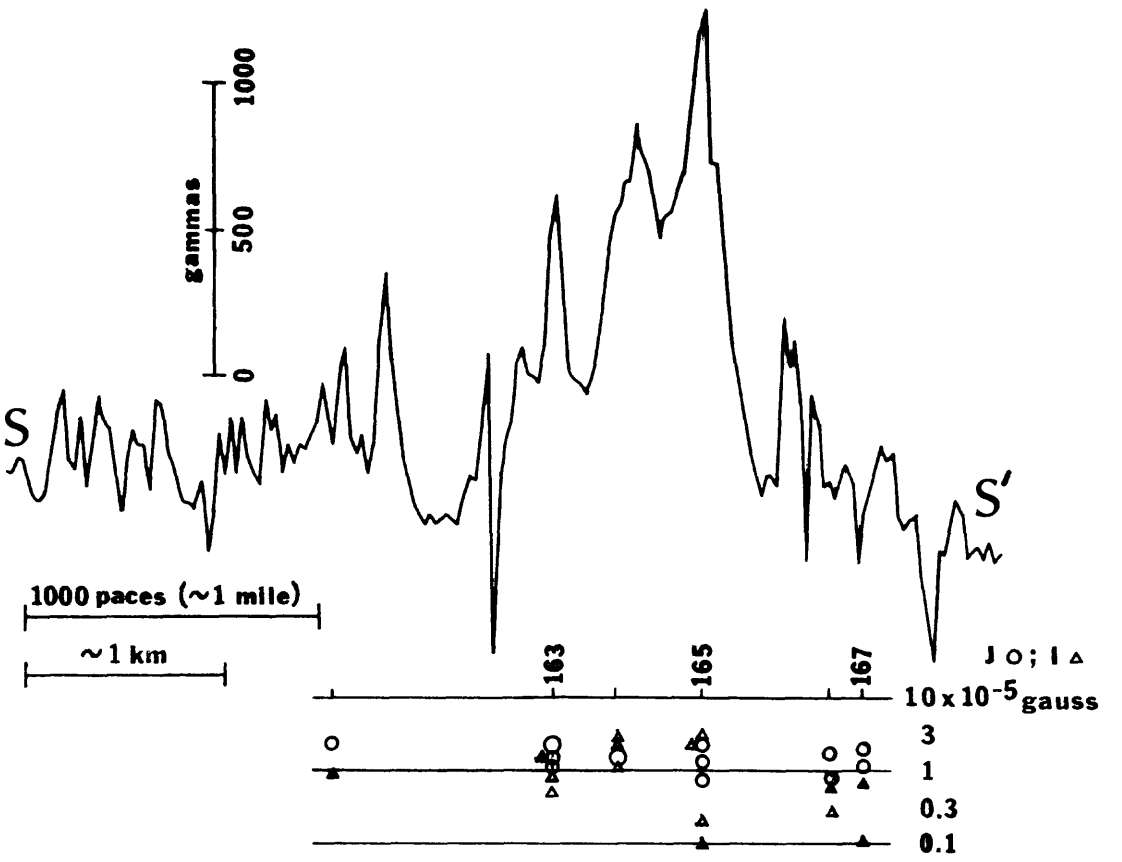
gammas
1000
500
0
S
S'
1000 paces (~1 mile)
~1 km
163
165
167
J ○; I △
10 x 10⁻⁵ gauss
3
1
0.3
0.1

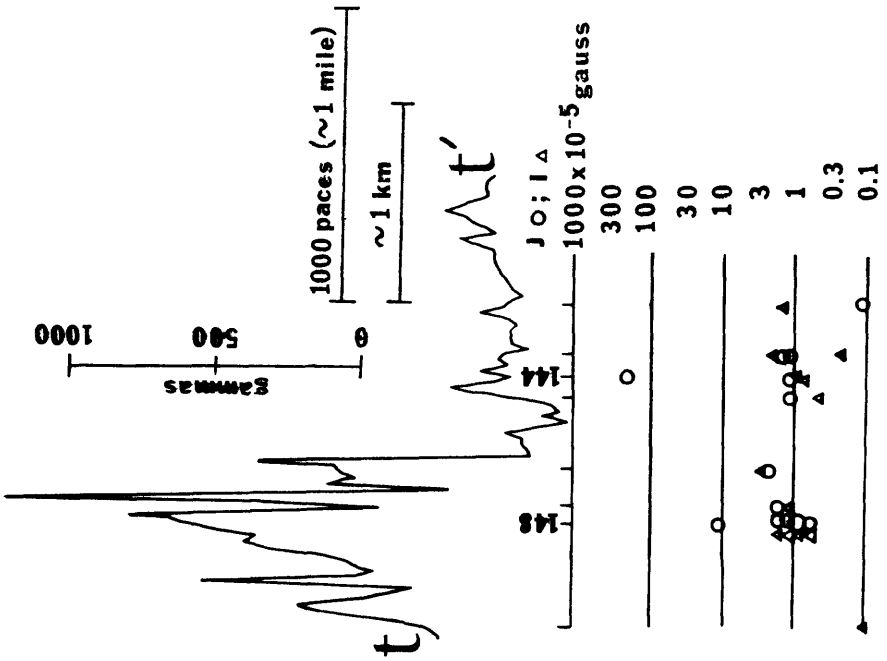
1000 paces (~1 mile)
~1 km
t'
J ○; I △
1000 x 10⁻⁵ gauss
300
100
30
10
3
1
0.3
0.1
144
148
t
0
500
1000
gammas

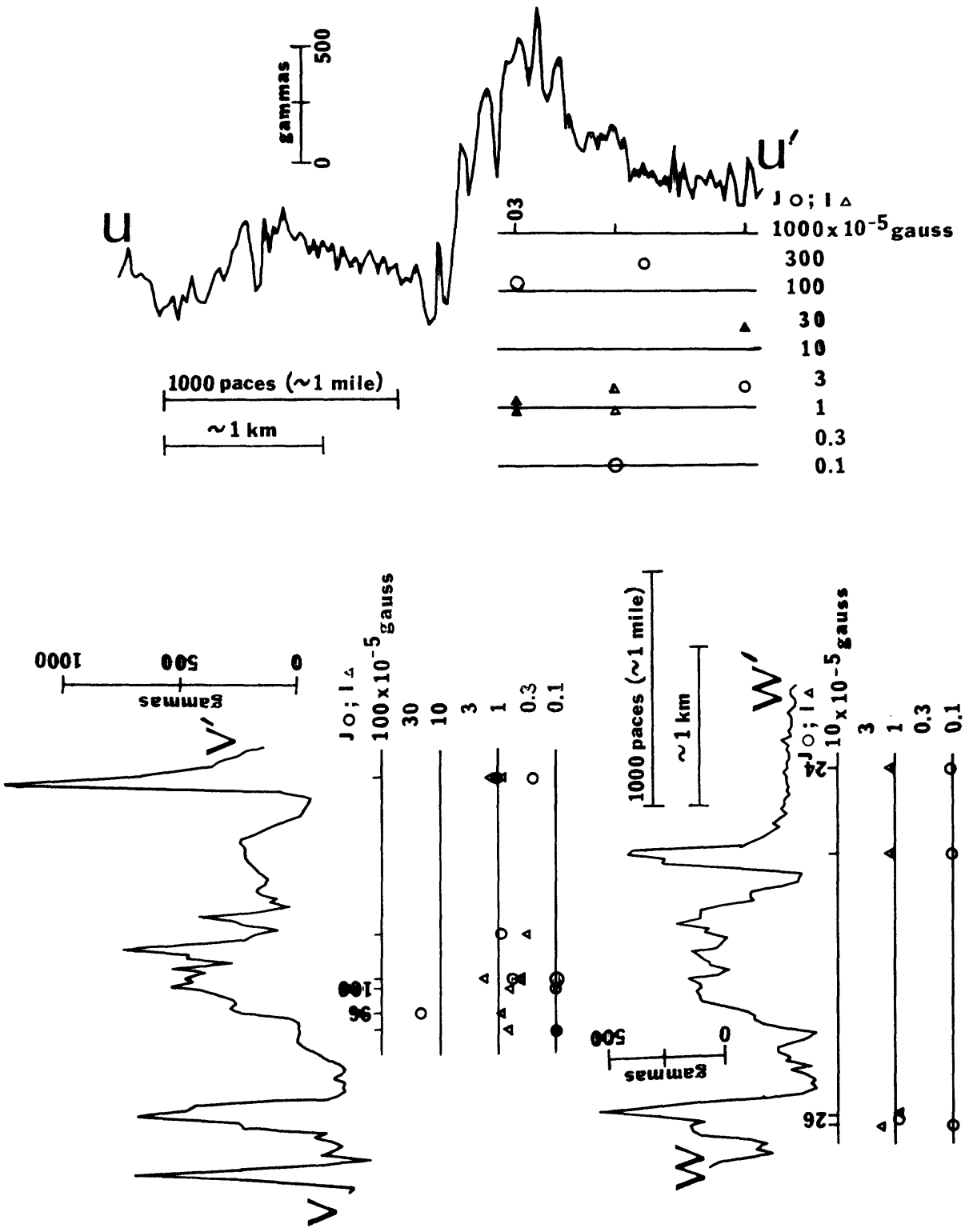
gammas
500
0
U
U′
J ○; I △
03
1000 x 10-5 gauss
300
100
30
10
3
1
0.3
0.1
1000 paces (~1 mile)
~1 km
V′
V
W′
W
1000
500
0
96
100
24
26

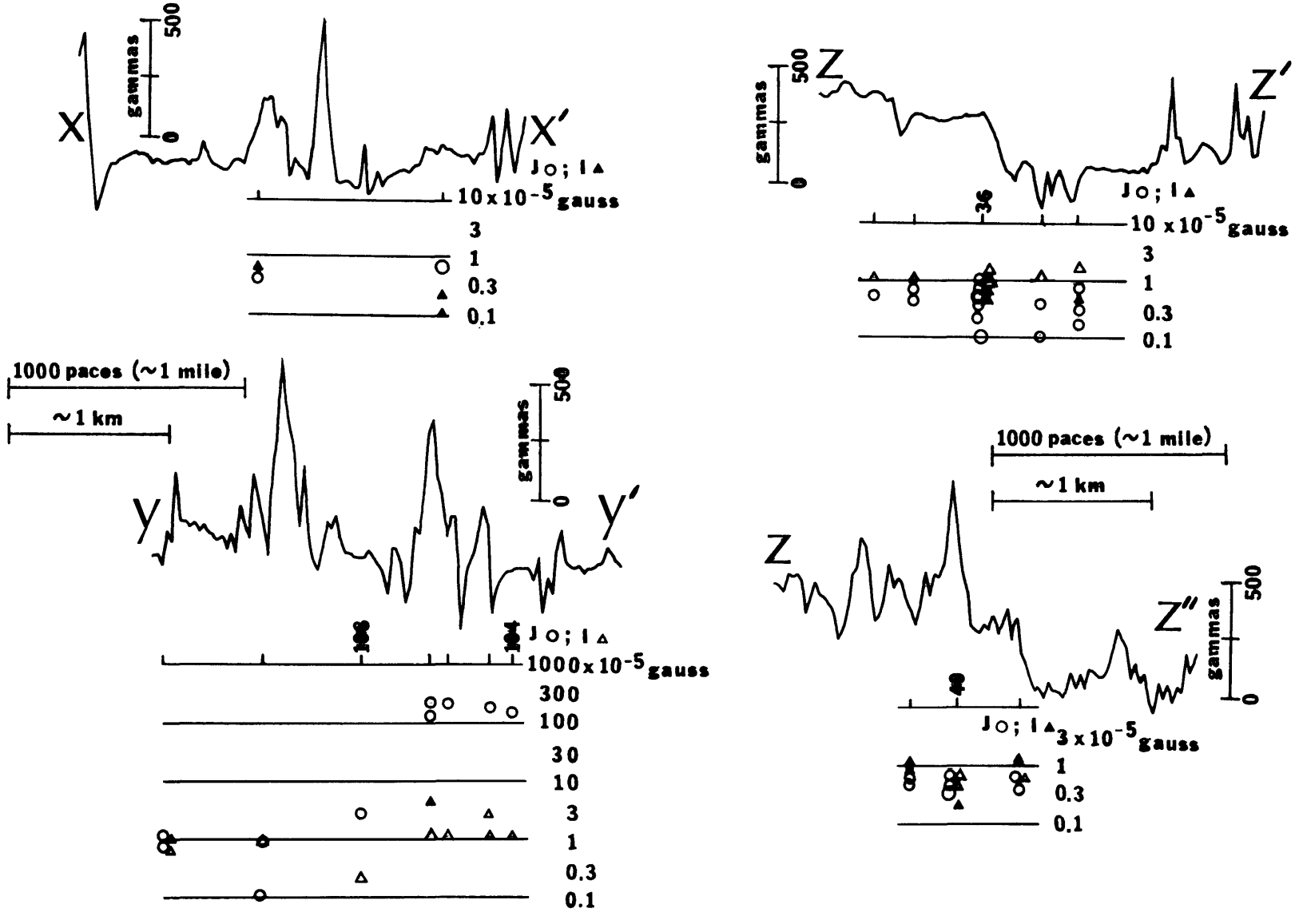
X
X′
gammas
500
0
J ○; I ▲
10 x 10⁻⁵ gauss
3
1
0.3
0.1
Z
Z′
-36
10 x 10⁻⁵ gauss
1000 paces (~1 mile)
~1 km
y
y′
1000 x 10⁻⁵ gauss
300
100
30
10
3
1
0.3
0.1
Z
Z″
3 x 10⁻⁵ gauss

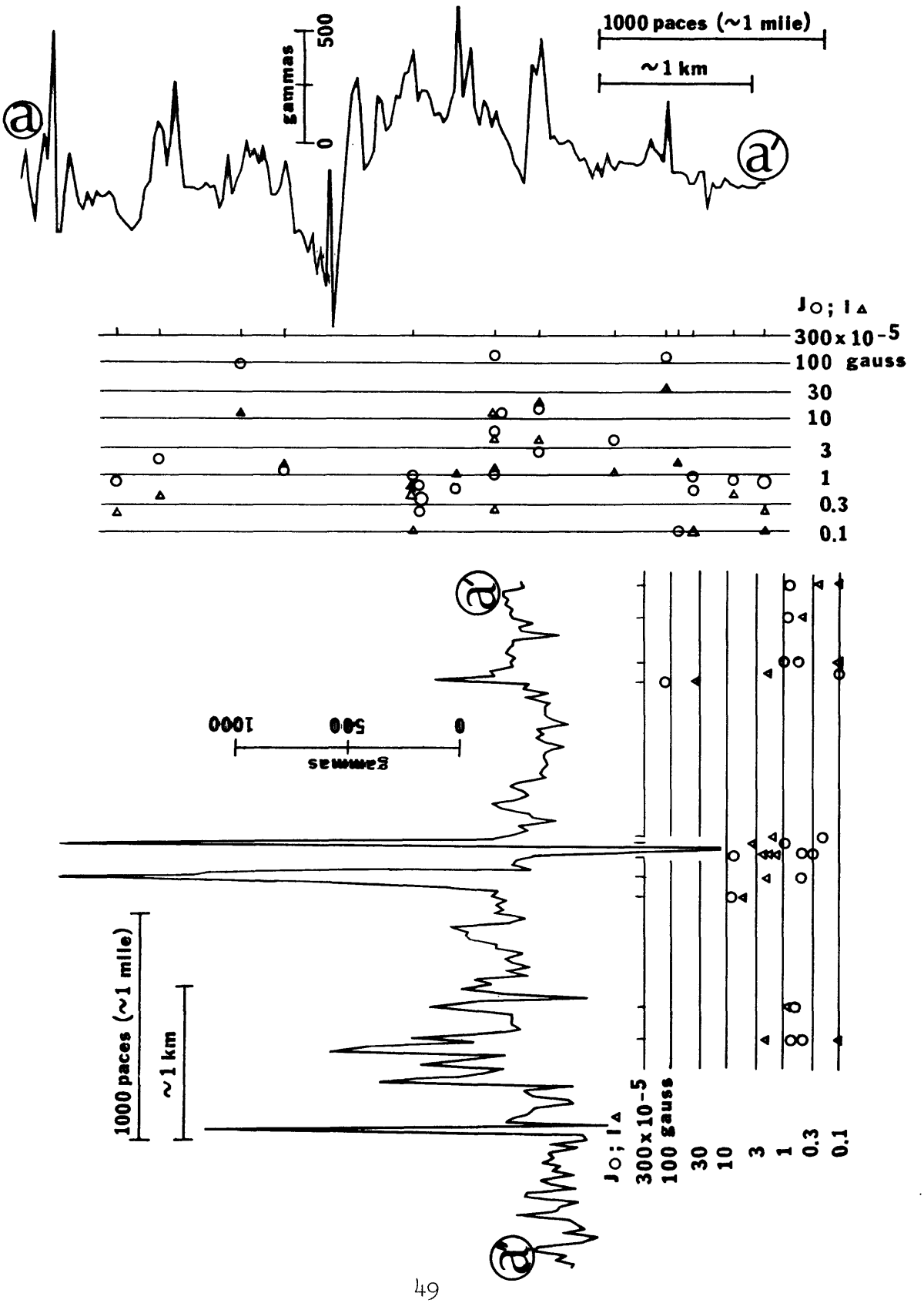
a
a'
gammas
500
0
1000 paces (~1 mile)
~1 km
J○; I△
300x10-5
100 gauss
30
10
3
1
0.3
0.1

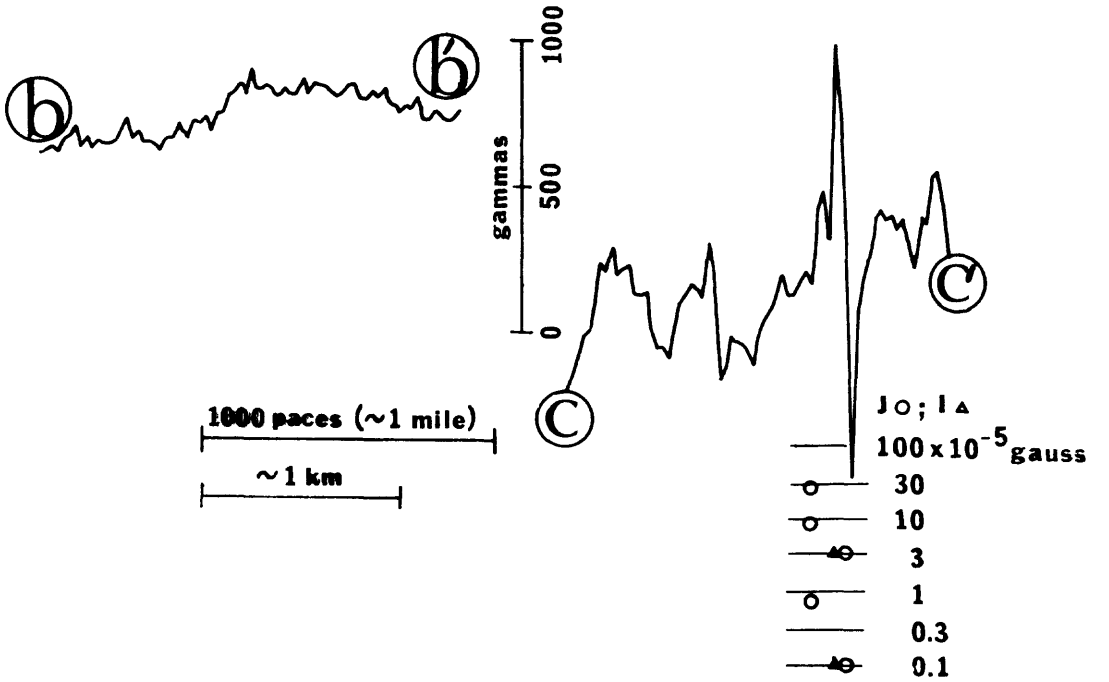
b
b'
c
c'
1000
500
0
gammas
1000 paces (~1 mile)
~1 km
J ○ ; I △
100 x 10⁻⁵ gauss
30
10
3
1
0.3
0.1

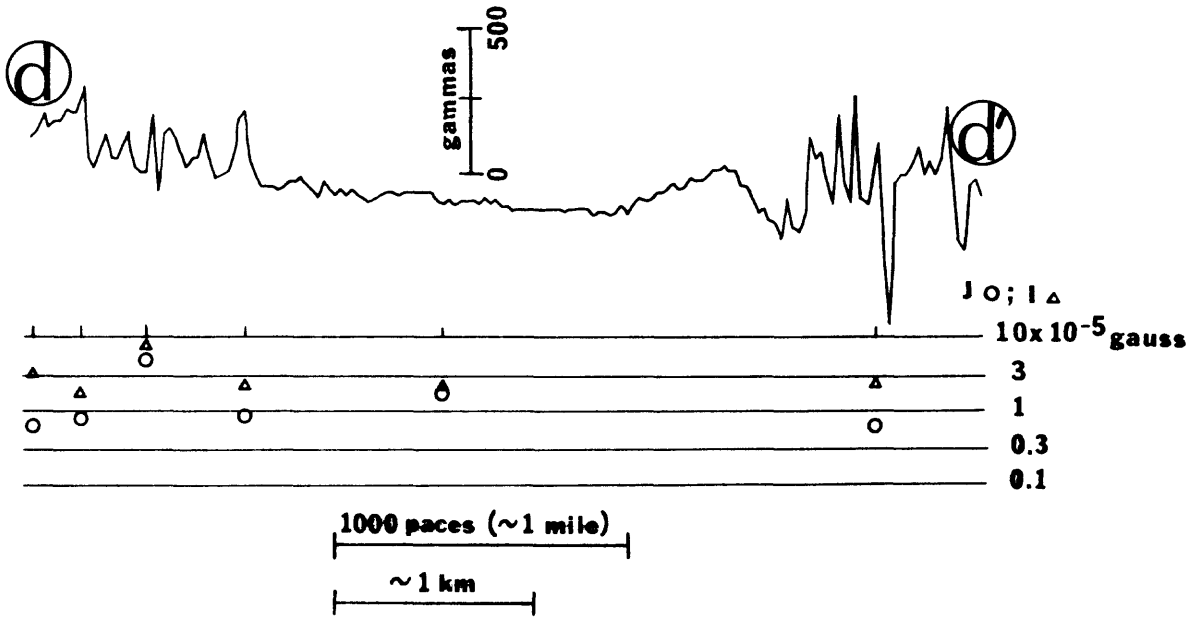
d
d'
500
0
gammas
J ○ ; I △
10 x 10⁻⁵ gauss
3
1
0.3
0.1
1000 paces (~1 mile)
~1 km

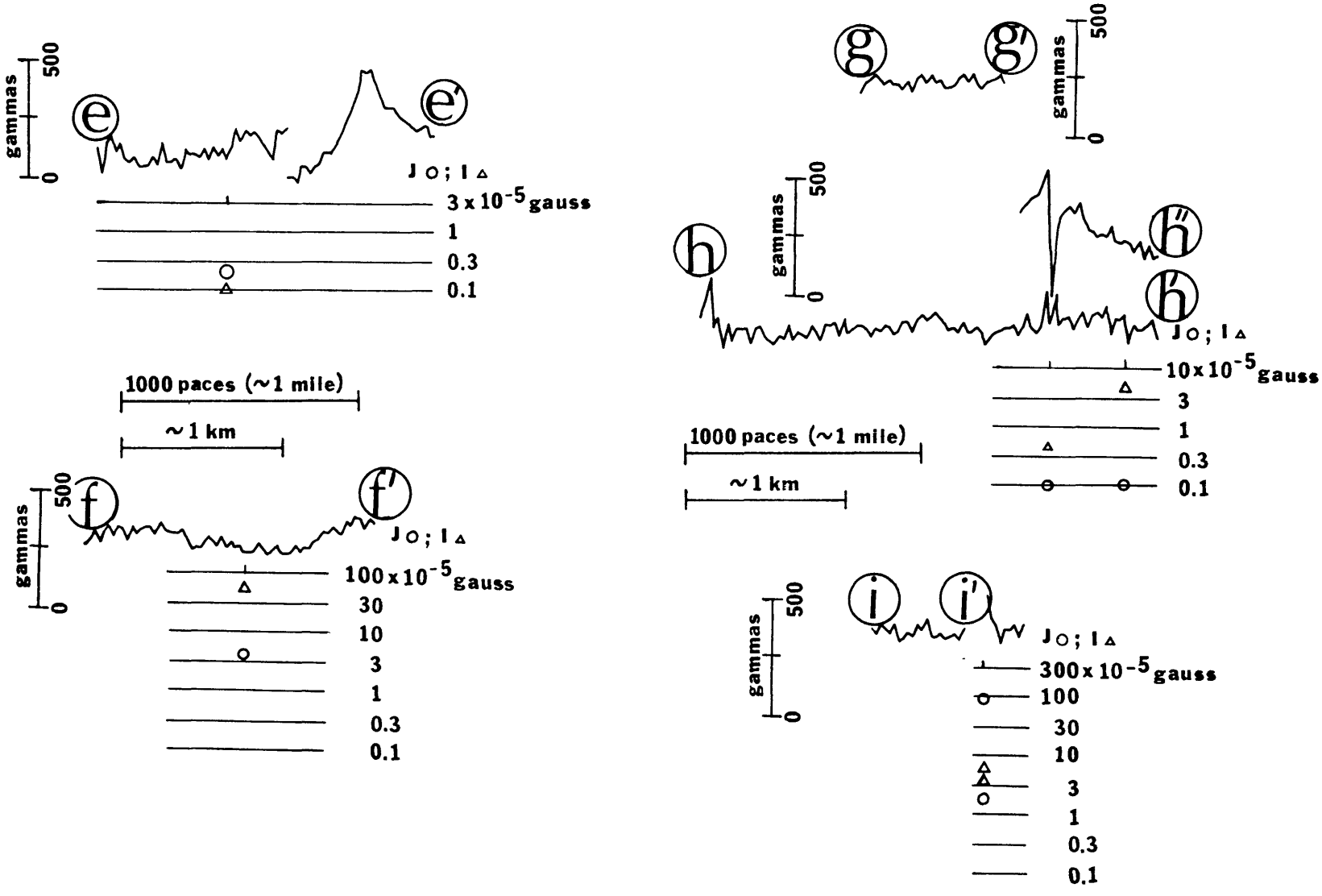
gammas
500
0
e
e'
J ○; I △
3 x 10-5 gauss
1
0.3
0.1
1000 paces (~1 mile)
~1 km
f
f'
100 x 10-5 gauss
30
10
3
1
0.3
0.1
g
g'
h
h''
h'
10 x 10-5 gauss
i
i'
300 x 10-5 gauss
100

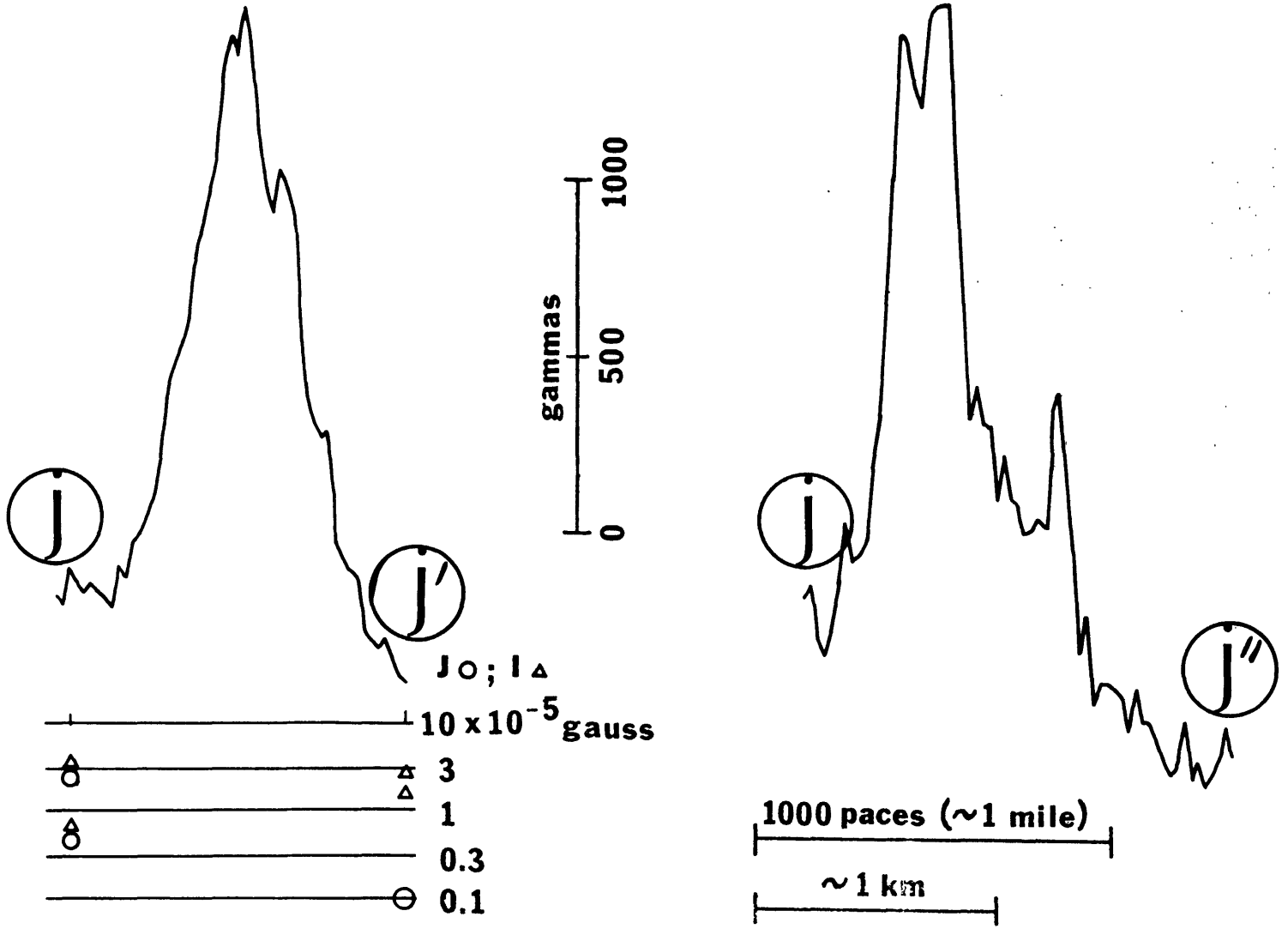
J
J′
J″
1000
500
0
gammas
J ○ ; I △
10 x 10⁻⁵ gauss
3
1
0.3
0.1
1000 paces (~1 mile)
~1 km